Study of Precipitate Evolution During Aging of IN617 Superalloys

M.Tech. Thesis

By

Adi Raj

(2302105022)

MTech - Metallurgical Engineering

DEPARTMENT OF METALLURGICAL ENGINEERING AND MATERIALS SCIENCE (MEMS)
INDIAN INSTITUTE OF TECHNOLOGY INDORE

MAY 2025

Study of Precipitate Evolution During Aging of IN617 Superalloys

A THESIS

Submitted in partial fulfillment of the requirements for the award of the degree
of
Master of Technology

by
Adi Raj

DEPARTMENT OF METALLURGICAL ENGINEERING AND MATERIALS SCIENCE (MEMS)

INDIAN INSTITUTE OF TECHNOLOGY INDORE

MAY 2025

INDIAN INSTITUTE OF TECHNOLOGY INDORE

CANDIDATE'S DECLARATION

I hereby certify that the work which is being presented in the thesis entitled **Study of Precipitate Evolution During Aging of IN617 Superalloys** in the partial fulfillment of the requirements for the award of the degree of **MASTER OF TECHNOLOGY** and submitted in the **DEPARTMENT OF METALLURGICAL ENGINEERING AND MATERIALS SCIENCE (MEMS), Indian Institute of Technology Indore**, is an authentic record of my own work carried out during the time period from August 2023 to May 2025 under the supervision of **Dr. Abhijit Ghosh,** Assistant Professor, MEMS, Indian Institute of Technology Indore.

The matter presented in this thesis has not been submitted by me for the award of any other degree of this or any other institute.

Adi Raj 29/05/2025

Signature of the student with date
ADI RAJ

This is to certify that the above statement made by the candidate is correct to the best of my/our knowledge.

Abhijit Ghosh

Signature of the Supervisor of
M.Tech. thesis
(Dr. Abhijit Ghosh)

ADI RAJ has successfully given his M.Tech. Oral Examination held on **26th May 2025**.

Abhijit Ghosh

Signature(s) of Supervisor(s) of M.Tech. thesis
Date: 28/05/25

29/05/2025 Acting DPGC

Convener, DPGC
Date:

ACKNOWLEDGEMENTS

I would like to express my deepest gratitude to Dr. Abhijit Ghosh Sir, my supervisor at IIT Indore, for his invaluable guidance, encouragement, and support throughout the course of my M. Tech thesis.

I would also like to extend my heartfelt thanks to Pravin Kumar, who is a senior research scholar from my lab for his assistance and constructive feedback, Mr. Pranjal Shrimali and Mr. Mayur Dhake sir, which also played a significant role in the successful completion of this thesis.

I dedicate this work to my beloved parents, whose unwavering support, encouragement, and sacrifices have been the foundation of all my achievements.

Thank you all for being a part of this endeavor.

ABSTRACT

This thesis investigates the Evolution of precipitates during the thermal aging of IN617 superalloy, a nickel-based alloy extensively used in high-temperature environments such as gas turbines and power plants. The main objective is to understand how different aging conditions influence precipitate formation, microstructure, and mechanical properties, thereby aiding in the optimization of material performance and durability.

IN617 samples were subjected to controlled aging treatments at 650°C, 700°C, 750°C, and 800°C for periods ranging from 120 to 5000 hours. Standard metallographic preparation was followed by detailed characterization using optical microscopy, SEM, EDS, and XRD. Microhardness testing was also performed to link microstructural changes with mechanical behavior.

The results show that intermediate aging temperatures (700–750°C) favour the formation of fine $M_{23}C_6$ carbides and γ′ (Ni_3 (Al, Ti)) precipitates, which are distributed along grain boundaries and within grains. These precipitates significantly enhance hardness and strength. However, prolonged aging or higher temperatures lead to coarsening and partial dissolution of these phases, resulting in a reduction in hardness and the onset of over aging. XRD analysis confirms the progressive development of secondary phases, while EDS mapping reveals chromium and molybdenum enrichment at grain boundaries, supporting carbide formation. The γ-matrix remains stable and rich in nickel and cobalt.

A bell-shaped hardness trend is observed, with maximum values at optimal aging conditions and a decline at longer durations or higher temperatures. Compared to literature, the precipitation kinetics in this study are slightly delayed and over aging occurs earlier, likely due to initial microstructural differences. These findings emphasize the importance of precise heat treatment control to balance strength and long-term reliability.
This work deepens the understanding of precipitate evolution in IN617 during aging and provides practical recommendations for processing and service, directly benefiting the design and maintenance of high-temperature components.

TABLE OF CONTENTS

LIST OF FIGURES

ACRONYMS

Acronym	Full Form
AR	As Received
BHEL	Bharat Heavy Electricals Limited
CDM	Continuum Damage Mechanics
DSC	Differential Scanning Calorimetry
EBSD	Electron Backscatter Diffraction
EDS	Energy Dispersive X-Ray Spectroscopy
EDX	Energy dispersive x-ray (alternative to EDS)
GB	Grain Boundary
HAZ	Heat Affected Zone
HRTEM	High Resolution Transmission Electron Microscopy
MC	Metal Carbide (often TIC or similar in superalloy)
SEM	Scanning Electron Microscopy
STEM	Scanning Transmission Electron Microscopy
TEM	Transmission Electron Microscopy
USC	Ultra-Supercritical (as in USC Powerplant
XRD	X-Ray Diffraction

LIST OF TABLES

Chapter 1

Introduction

Nickel-based superalloys have become indispensable in modern high-temperature engineering applications due to their remarkable combination of mechanical strength, corrosion resistance, and microstructural stability. Among these, IN617 (Inconel 617) stands out as a leading material for components subjected to extreme environments, such as gas turbines, petrochemical processing units, and advanced nuclear reactors. The superior performance of IN617 at elevated temperatures is primarily attributed to its complex microstructure, which is stabilized by a carefully balanced composition of nickel, chromium, cobalt, and molybdenum. However, the long-term reliability of IN617 in service conditions is closely linked to the evolution of its microstructure-particularly the behavior of precipitate phases during thermal aging. such as carbides ($M_{23}C_6$, M_6C) and intermetallic phases (γ') play a crucial role in strengthening IN617 by impeding dislocation movement and stabilizing grain boundaries. Over prolonged exposure to high temperatures, these precipitates undergo significant morphological and compositional changes, which in turn influence the alloy's mechanical properties, including creep resistance, hardness, and toughness. Understanding the kinetics and mechanisms of precipitate evolution during aging is therefore essential for predicting the service life of IN617 components and for developing strategies to enhance their performance. Despite extensive research on IN617, several knowledge gaps remain regarding the precise sequence of microstructural transformations during aging, the interplay between different precipitate phases, and their impact on mechanical behavior. Most existing studies have focused on short-term aging or have not systematically correlated microstructural changes with property degradation over extended periods.

Furthermore, as IN617 is increasingly considered for next-generation nuclear reactors, where components are expected to operate reliably for decades, there is a pressing need for comprehensive data on its long-term stability. This thesis aims to investigate the microstructure evolution of precipitates in IN617 during isothermal aging, with a focus on characterizing nature, distribution, and growth kinetics of key precipitate phases. By employing advanced characterization techniques such as scanning electron microscopy (SEM), transmission electron microscopy (TEM), and X-ray diffraction (XRD), this study

seeks to establish clear correlations between aging conditions, microstructural changes, and mechanical properties. The insights gained will contribute to a deeper understanding of the aging behavior of IN617 and provide valuable guidance for material selection, component design, and life prediction in high-temperature applications.[1]

1.1 High-temperature applications and the need for robust materials

The ongoing pursuit of higher efficiency and lower environmental impact in power generation has driven the development of advanced ultra-supercritical (USC) power plants, which operate at steam temperatures up to 750 °C and pressures as high as 37.5 MPa. These extreme service conditions place unprecedented demands on structural materials, necessitating not only exceptional high-temperature strength but also sustained resistance to creep, oxidation, and corrosion over prolonged service periods. Traditional materials, which have typically been used in less severe environments and for shorter durations, are inadequate for these new requirements. As a result, nickel- based superalloys, particularly INCONEL 617, have emerged as leading candidates for critical components such as boilers and heat exchangers in USC plants due to their superior combination of high-temperature strength, corrosion resistance, and creep resistance. However, the transition from their established applications-such as turbine engines in the aerospace industry, where exposure times are shorter and environments less corrosive-to USC power plant service requires a deeper understanding of their long- term microstructural evolution. For these demanding applications, the forecasted requirements include a minimum creep strength of 100 MPa after 100,000 hours of service. Despite their promise, there is a lack of widespread microstructural data for nickel-based alloys after such extended exposure, making it essential to investigate how their microstructure evolves under simulated service conditions. This includes understanding the behavior of key strengthening precipitates, such as γ' and various carbides, which play a crucial role in the alloy's performance. Consequently, both experimental characterization and advanced modelling, such as continuum damage mechanics (CDM), are necessary to predict and validate the long-term behavior of these materials, ensuring their reliability and safety in next-generation high-temperature energy systems.

1.2 Ni-based superalloys and their advantages

Nickel-based superalloys have become the materials of choice for advanced high-temperature applications, particularly in the context of ultra-supercritical (USC) power plants where steam temperatures can reach up to 750°C and pressures as high as 37.5 MPa. These demanding service conditions require materials that not only possess excellent high-temperature strength but also maintain their integrity under prolonged exposure to aggressive environments. Ni-based superalloys, such as INCONEL 617, are specifically engineered to meet these requirements, offering a superior combination of mechanical strength, creep resistance, and exceptional resistance to oxidation and corrosion. Historically, these alloys have found extensive use in the aerospace industry, especially in turbine engines, due to their ability to withstand short-term, high-stress environments. However, the transition to power generation applications introduces new challenges, including the need for reliable performance over service lifetimes that can extend to 100,000 hours or more [1] [2].

A key advantage of Ni-based superalloys lies in their complex microstructure, which can be tailored through alloying and thermo-mechanical treatments. INCONEL 617, for example, is a solid solution strengthened alloy that is typically used in the solution annealed condition. Its microstructure is characterized by the presence of various strengthening precipitates, including γ' (gamma prime), $M_{23}C_6$, M_6C, and MX carbides, which play a critical role in hardening the material and impeding dislocation movement. These precipitates are distributed both within grains and along grain boundaries, providing a balance between strength and ductility. The stability of these phases during long-term exposure is essential for maintaining mechanical properties such as creep strength and hardness.

Another significant benefit of Ni-based superalloys is their ability to form a protective oxide layer on their surface, which enhances their resistance to high-temperature oxidation and corrosion. This is particularly important in USC power plant environments, where exposure to steam and corrosive gases is continuous. The paper highlights that the microstructural evolution of IN617 under service conditions- including changes in precipitate size, volume fraction, and distribution-can be effectively characterized and modelled, providing valuable input for predicting long- term performance. Advanced techniques such as electron backscatter diffraction (EBSD), scanning electron microscopy (SEM), and energy-dispersive X-ray spectroscopy (EDX) are employed to analyse these microstructural features in detail.

Furthermore, the ability to model and forecast the behaviour of Ni-based superalloys using approaches like continuum damage mechanics (CDM) provides a powerful tool for designing alloys with improved performance and reliability. The combination of experimental characterization and predictive modelling enables the optimization of alloy composition and processing, ensuring that Ni-based superalloys like INCONEL 617 continue to meet the evolving demands of high-temperature energy systems. Overall, the unique blend of high-temperature strength, microstructural stability, and environmental resistance makes Ni-based superalloys indispensable for the next generation of power plant technologies and other critical high-temperature applications.

1.3 Composition, properties, and industrial role

INCONEL 617 (IN617) is a nickel-based superalloy specifically engineered for high-temperature applications, such as those found in advanced ultra-supercritical (USC) power plants. Its nominal chemical composition includes high levels of nickel (balance), chromium (24%), cobalt (10%), and molybdenum (8%), with smaller amounts of aluminum, titanium, and carbon, among other elements. This composition provides IN617 with a unique combination of high-temperature strength, excellent resistance to oxidation and corrosion, and superior creep resistance, making it a primary candidate material for critical components like boilers and heat exchangers operating at steam temperatures up to 750 °C and pressures of 35–37.5 MPa [3]. IN617 is a solid-solution strengthened alloy, typically used in the solution-annealed condition, but it also derives significant hardening from the presence of γ' phase and carbides such as $M_{23}C_6$, M_6C, and MX. These precipitates are distributed both within grains and along grain boundaries, playing a crucial role in impeding dislocation motion and enhancing the alloy's mechanical performance during prolonged high-temperature service. The alloy's microstructural stability and resistance to degradation under extreme conditions make it highly suitable for demanding power generation environments, where long-term reliability and efficiency are essential. As the industry moves toward higher efficiency and lower emissions, IN617's robust properties and proven performance position it as a key material in the next generation of energy systems.

1.4 The critical role of precipitates in determining alloy performance

Precipitates play a fundamental role in determining the high-temperature performance of INCONEL 617, especially in demanding environments such as ultra-supercritical (USC) power plants. The alloy's microstructure is characterized by a range of precipitate phases, including γ', $M_{23}C6$, M_6C, and MX carbides, which are present both in the as received and aged conditions. These precipitates are crucial for hardening the material, as they impede dislocation motion and thus enhance the creep resistance and mechanical strength of the alloy. The distribution, size, and volume fraction of these precipitates evolve during long-term exposure to elevated temperatures, directly influencing the material's ability to maintain its properties over time. For instance, finely dispersed γ' and carbides within the grains contribute to strengthening, while carbides at grain boundaries can both reinforce and, if coarsened or excessively concentrated, potentially embrittle the alloy. The paper emphasizes that the stability and morphology of these phases are key factors in ensuring that IN617 meets the stringent requirements for creep strength-such as a minimum of 100 MPa after 100,000 hours of service-set for USC applications [3].

Microstructural analysis in the study reveals that after creep exposure at 650–750°C for up to 20,000 hours, the grain structure remains stable, and the main precipitate types persist, although their size and spacing may change. The presence of precipitates like MX (often Ti(N)) and $M_{23}C_6$ at grain boundaries, confirmed through SEM and EDX analyses, highlights their role in controlling grain boundary sliding and cavitation during creep. The quantification of phase fractions, mean particle size, and inter-particle spacing is not only essential for understanding the alloy's current state but also serves as critical input for predictive models, such as the continuum damage mechanics (CDM) approach used in the paper.

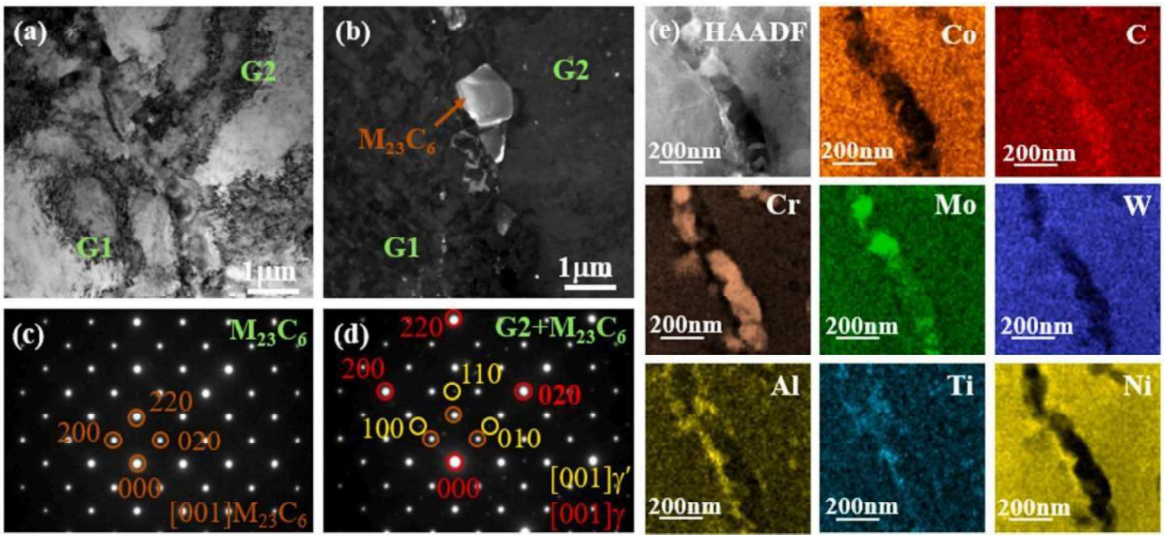

Fig.1.1. TEM images of the sample after 1500 h of aging: (a) bright-field image showing precipitates at grain boundary, (b) dark-field image of $M_{23}C_6$ carbide coherently aligned with grain G2 at the grain boundary, (c) selected area electron diffraction (SAED) pattern from $M_{23}C_6$ carbide shown in (b), (d) selected electron diffraction pattern illustrating the cube-on-cube orientation relationship between grain G2 and $M_{23}C_6$ carbide. (e) HAADF-STEM micrograph of the carbide with corresponding EDS (Energy Dispersive X-ray Spectroscopy) mapping images [4].

These models rely on accurate microstructural data to forecast long-term mechanical behavior, further underscoring the importance of precipitate characterization. Overall, the evolution and stability of precipitates are central to the alloy's ability to resist deformation and failure during prolonged high-temperature service, making their study essential for the continued development and application of IN617 in advanced energy systems. In summary, the evolution, distribution, and stability of precipitates such as γ', $M_{23}C_6$, M_6C, and MX are central to the exceptional high-temperature performance of IN617. The present investigation demonstrates that these phases, through their hardening effect and their ability to impede dislocation motion, are vital for maintaining the alloy's creep resistance and structural integrity during long-term service. Quantitative microstructural analysis, including measurements of phase fraction, particle size, and inter-particle spacing, provides essential insight into how these precipitates change under different thermo-mechanical treatments and aging conditions. The integration of such detailed microstructural data into predictive models, like continuum damage mechanics, further underscores the importance of understanding precipitate behavior for accurate forecasting of alloy performance. Ultimately, the ability to characterize and control precipitate evolution is key to optimizing IN617 for demanding applications in advanced power generation, ensuring both reliability and longevity in service.

1.5 How aging affects microstructure and properties

Aging of IN617 at elevated temperatures (650–760°C) induces significant microstructural changes that directly influence its mechanical properties. During short- term aging (200–1,000 hours), $M_{23}C_6$ and M_6C carbides precipitate rapidly, forming intragranular and along grain boundaries, while γ′ phase (Ni_3(Al, Ti)) nucleates heterogeneously at twin boundaries and carbide-matrix interfaces.

These precipitates enhance yield strength (e.g., from 314 MPa to 532 MPa at 650°C after 5,300 hours) through precipitation hardening but reduce ductility (62% to 42%) and Charpy impact energy (150J to 60J) due to embrittlement.

Long-term aging (5,000–20,000 hours) leads to coarsening of carbides and γ′ dissolution, particularly at 750°C, where carbides aggregate into "sunburst" clusters and grain boundaries develop serrations, weakening intergranular cohesion.[5]

The carbide-depleted zone beneath the oxide layer expands with aging time, driven by chromium migration to support surface oxidation, further reduce creep resistance.

(a): Shows a low-magnification microstructure where annealing twins are visible within the grains, indicated by the straight, mirror-like boundaries characteristic of twin boundaries.

(b):At higher magnification, the image highlights the presence of $M_{23}C_6$ carbide precipitates decorating both the grain/twin boundaries and within the grains, with the twin boundary clearly marked and fine precipitates distributed along it.

(c): Further magnified, this image focuses on the twin boundary, showing dense, nanoscale $M_{23}C_6$ carbides precisely aligned along the boundary, demonstrating preferential precipitation at these special interfaces At 750°C, γ′ dissolution necessitates a threshold stress (~65 MPa) to counteract dislocation shearing during creep, while aging at 650°C retains γ′ stability, sustaining work hardening rates. Hardness initially increases with carbide and γ′ precipitation but declines after 5,000 hours due to over-aging and precipitate coarsening.

Microstructural stability varies with temperature: grain size remains stable (123–176 μm after 20,000 hours), but carbide redistribution and γ′ evolution dominate degradation.[4] [2].

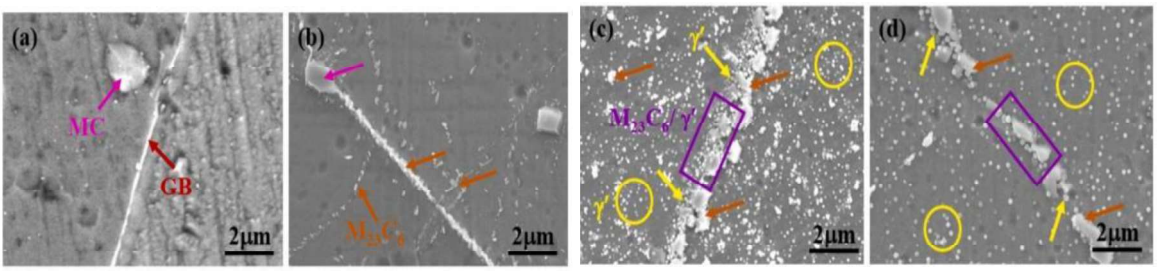

Fig. 1.2. SEM images illustrating: (a) grain boundary carbides in the microstructure after solution treatment, and the growth of continuous grain boundary phases after aging at 760 ◦C for various durations: (b) 20 h, (c) 1500 h, and (d) 6000 h [4].

These changes underscore the trade-off between short-term strengthening and long-term embrittlement, critical for applications in advanced reactors and power plants where IN617 must withstand decades of service. Overall, the aging-induced microstructural evolution in IN617 highlights the delicate balance between strengthening and degradation mechanisms. While initial precipitation of carbides and γ′ phases significantly enhance mechanical strength and creep resistance, prolonged exposure leads to coarsening, phase dissolution, and embrittlement that compromise long-term performance. Understanding these transformations is essential for optimizing heat treatment processes and predicting service life in high-temperature applications. Continued research combining experimental characterization and predictive modelling will be crucial to improving alloy design and ensuring the reliability of IN617 in demanding environments such as ultra-supercritical power plants and advanced nuclear reactors.

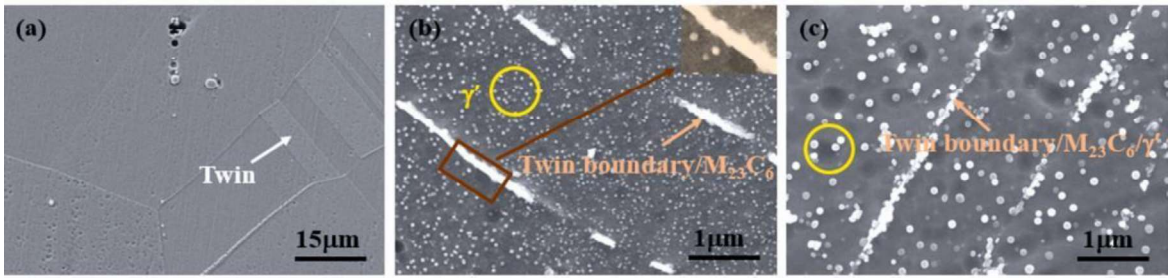

Fig. 1.3. Microstructures of the samples under different conditions: (a) as-solution treated; (b) aged for 300 h; (c) aged for 1500 h.[4].

(a): Shows a low-magnification microstructure (15μm scale) with clearly visible annealing twins within the grains, indicated by the straight, parallel boundaries that are characteristic of coherent twin boundaries in the material. (b): At higher magnification (1μm scale), the image reveals $M_{23}C_6$ carbide precipitates decorating the twin boundary, with the circled regions highlighting specific areas where these carbides have preferentially nucleated along the twin interface and (c): Further magnified view (1μm scale) focusing on the twin

boundary decorated with $M_{23}C_6$ carbides, showing dense, fine precipitates aligned along the boundary and demonstrating the preferential precipitation behavior at these special grain boundary interfaces Toughness is not yet fully established, particularly for service times exceeding 10,000 hours. Addressing these gaps will require more systematic long-term studies, advanced characterization techniques, and improved microstructural modelling to accurately predict the performance and reliability of IN617 in demanding high-temperature environments.

1.6 Current knowledge gaps in precipitate evolution during aging

Vividly illustrate the evolving microstructure of IN617 during long-term aging yet also reveal important knowledge gaps. While the images show clear differences in precipitate distribution and γ′ coarsening between ST and SST alloys, the underlying mechanisms that govern these differences-such as the role of elemental partitioning, the interplay between carbides and γ′, and the influence of initial microstructure-remain insufficiently understood. Additionally, the transition in γ′ morphology and the rate of coarsening highlight the need for deeper insight into diffusion processes and phase stability over extended service times. These visualizations emphasize that, despite progress, the precise pathways and controlling factors of precipitate evolution during aging in IN617 require further systematic investigation. Another unresolved issue is the relationship between precipitating evolution and mechanical properties. While hardness increases with the precipitation of carbides and γ′ during early and intermediate aging, a decline is observed after prolonged exposure, likely due to precipitate coarsening and embrittlement at grain boundaries. Furthermore, the redistribution of alloying elements (like Cr, Mo, Al, and Ti) during aging, and their role in stabilizing or destabilizing different precipitate phases, is still not fully quantified, especially under varying service conditions and chemistries.

1.7 Summary of the thesis

The primary objective of this thesis is to systematically investigate the precipitation behavior of the γ′ phase and other secondary phases in IN617 alloy subjected to various aging conditions relevant to high-temperature industrial applications. This research aims to thoroughly characterize the types, morphology, and spatial distribution of precipitates-including γ′, $M_{23}C_6$, M_6C, and MC carbides-formed during both short-term and long-term

aging at different temperatures. A key goal is to elucidate the kinetics of nucleation, growth, coarsening, and possible dissolution of these phases, and to determine how these processes are influenced by factors such as temperature, aging duration, and initial microstructure. The study will also focus on the evolution of precipitate size, volume fraction, and their distribution within grains and along grain boundaries, as these features critically affect the mechanical performance of IN617. By employing advanced characterization techniques such as SEM, TEM, and EDS, the research seeks to provide a detailed understanding of phase stability and the interactions between different precipitate types. Another important objective is to correlate the observed microstructural changes with variations in key mechanical properties, including hardness, tensile strength, creep resistance, and toughness, thereby clarifying the mechanisms by which precipitate evolution contributes to strengthening or embrittlement. Furthermore, the thesis aims to assess the role of elemental redistribution-particularly of Cr, Mo, Al, and Ti-during aging, and its impact on the stability and transformation of secondary phases. The goal is to generate insights that will inform the optimization of aging treatments for IN617, enabling improved performance and reliability in demanding high-temperature environments such as ultra- supercritical power plants and advanced nuclear reactors. Through this comprehensive investigation, the thesis aspires to address current knowledge gaps in the field and provide a foundation for predictive modelling of long-term microstructural evolution and mechanical degradation in Ni-based superalloys.

Chapter 2

Literature Survey

IN617, also known as Inconel 617, emerged from the need for materials capable of maintaining high strength and oxidation resistance at elevated temperatures, particularly for use in advanced gas turbines and power generation systems. Its development was driven by the rapid progress in high-temperature engineering during the mid-20th century, as industries sought alloys that could withstand the extreme conditions found in both aircraft and land-based gas turbines. The alloy was specifically engineered as a solid- solution strengthened nickel-chromium-cobalt-molybdenum material, with significant additions of aluminium to further enhance its oxidation resistance. The combination of these elements provided IN617 with a unique balance of high-temperature strength, metallurgical stability, and resistance to a wide range of corrosive environments [6]. This made it particularly attractive for critical components such as combustion cans, ducting, and transition liners, where both mechanical performance and durability against oxidation and corrosion were essential. IN617's introduction allowed designers to push the boundaries of operating temperatures in turbines and boilers, supporting the development of more efficient and powerful energy systems. Its versatility also led to applications in chemical processing, nitric acid production, heat-treating equipment, and, more recently, as a candidate material for components in fossil-fueled and nuclear power plants. The alloy's robust performance at temperatures above 980°C (1800°F) and its ability to be readily formed and welded by conventional techniques further cemented its role in these demanding industries. IN617 stands out among high-temperature alloys due to its exceptional combination of mechanical strength, oxidation resistance, and metallurgical stability at elevated temperatures. Capable of maintaining its strength above 980°C, IN617 is particularly suited for demanding environments such as gas turbines, power generation systems, and advanced reactors. Its high chromium and aluminium content enable the rapid formation of a protective oxide layer, granting the alloy outstanding resistance to oxidation and corrosion in both oxidizing and reducing atmospheres. Additionally, IN617 demonstrates excellent resistance to carburization and chloride-induced stress corrosion cracking, which is vital for chemical processing and petrochemical applications. The alloy's microstructure remains stable even during prolonged exposure to high temperatures, preserving its mechanical properties and extending component life [7]. IN617 is also valued for its good

fabricability and weldability, allowing it to be easily formed and joined using conventional methods. Its ability to retain ductility and resist fatigue and creep under cyclic loading further enhances its reliability in service. Collectively, these unique properties make IN617 a preferred material for critical components operating in extreme and corrosive environments. IN617 is widely used in high-temperature and corrosive environments due to its exceptional mechanical strength, oxidation resistance, and metallurgical stability.

Its primary applications include critical components in both aircraft and land-based gas turbines-such as combustion cans, transition liners, and ducting-where it withstands extreme temperatures and stresses. In power generation, IN617 is employed in both fossil- fuel and nuclear plants for heat exchangers, steam reformer tubes, and ultra-supercritical boiler tubes, owing to its ability to retain strength and resist corrosion at elevated temperatures. The alloy is also favoured in the petrochemical industry for catalyst grids support nitric acid production, heat-treating baskets, and reduction boats for molybdenum refining, as well as in industrial furnace components and high-performance piping system. Despite these advantages, challenges persist in these demanding applications. IN617 can be difficult to machine and fabricate due to its high strength and work-hardening characteristics, leading to increased manufacturing costs and shorter tool life. Long-term exposure to extreme temperatures can result in microstructural changes, such as precipitate coarsening and phase instability, which may degrade mechanical properties over time.[3] Additionally, the alloy's high cost and the need for specialized welding and joining techniques can limit its widespread adoption in cost-sensitive projects. These challenges necessitate ongoing research and careful engineering to optimize the performance and longevity of IN617 components in service.

2.1 Mechanical properties of IN617 Superalloy

The mechanical properties of IN617 superalloy are closely linked to its microstructural evolution during prolonged high-temperature service. The alloy's strength is primarily derived from solid solution strengthening by elements like cobalt and molybdenum, as well as precipitation of secondary phases such as γ' and carbides ($M_{23}C_6$ and M_6C). The γ' phase, which remains present even after 65,000 hours at 800°C, plays a crucial role in maintaining high-temperature strength by pinning dislocations and impeding grain boundary sliding. However, its volume fraction decreases with extended exposure, as observed in samples operated for 98,000 hours, indicating a gradual reduction in strengthening effect over time.

Carbide precipitation, particularly $M_{23}C_6$ at grain boundaries, significantly enhances creep resistance and overall mechanical stability, provided the carbides are well-dispersed and appropriately sized. The area fraction of carbides increases with service time, from 0.5% in the as-received state to 5.5% after 98,000 hours, contributing to sustained hardness and tensile strength. Interestingly, while $M_{23}C_6$ carbides increase with time, M_6C carbides decrease due to phase transformations, reflecting complex microstructural dynamics. Hardness and strength are highest in the 65,000-hour sample, but even after 98,000 hours, these values remain superior to the as- received condition, demonstrating the alloy's remarkable long-term stability. The presence of additional phases such as Ti(C, N) carbonitrides and minor δ phase further contributes to the alloy's mechanical robustness[2][8] Overall, IN617 exhibits excellent retention of mechanical properties under prolonged high-temperature exposure, making it a strong candidate for critical components in gas turbines and ultra-supercritical power plants.

The paper emphasizes several key mechanical properties of IN617 superalloy that make it highly suitable for long-term, high-temperature applications. Notably, IN617 demonstrates exceptional high-temperature strength, which is maintained through solid solution strengthening and the presence of γ' precipitates and carbides. Its outstanding creep resistance is attributed to the formation of $M_{23}C_6$ carbides at grain boundaries, which effectively hinder grain boundary sliding and enhance the alloy's stability during prolonged exposure to elevated temperatures.

The study also reports that the hardness of IN617 increases with service time, reaching peak values after intermediate durations due to optimal precipitation of strengthening phases, and remains higher than the as-received condition even after 98,000 hours of operation.

Additionally, the alloy retains its tensile strength over extended periods, with the microstructural stability provided by the persistence of γ' phase and the evolution of carbides. While the paper primarily focuses on strength and hardness, it also notes that IN617 maintains adequate ductility and toughness, ensuring reliable performance in demanding environments.

These mechanical properties collectively underline the alloy's suitability for critical components in gas turbines and ultra-supercritical power plants, where sustained mechanical integrity under high thermal stress is essential.

2.2 Microstructure of IN617 Superalloy

The microstructure of IN617 superalloy, as detailed in the referenced paper, is primarily composed of an austenitic matrix with a complex distribution of secondary phases that are crucial to its high-temperature performance. In the base metal, the alloy exhibits a pronounced banded structure of austenitic grains interspersed with secondary phases both along grain boundaries and within the grains themselves.

The most significant of these are $M_{23}C_6$ carbides, rich in chromium and molybdenum, which preferentially precipitate at grain boundaries and play a vital role in enhancing creep resistance and stabilizing the grain structure during prolonged high-temperature exposure. Additionally, larger polygonal Ti(C, N) carbonitride particles, approximately 10 μm in size, are observed within the grains, contributing further to the alloy's mechanical stability. The heat- affected zone (HAZ) adjacent to the weld area displays coarsened secondary phases and a lamellar structure enriched with chromium and molybdenum along the grain boundaries. In the weld metal, the microstructure is fully austenitic with a dendritic morphology, and fine precipitates are uniformly dispersed throughout the matrix.

The as-received alloy also contains γ′-Ni_3 (Al, Ti) phase and other carbides such as M_6C and MC, which evolve and redistribute with long-term service at elevated temperatures. Importantly, no significant elemental segregation is detected in the HAZ, while in the weld metal, minor nickel and cobalt depletion may occur near solidification grain boundaries, with chromium and molybdenum remaining evenly distributed. This intricate and stable microstructural framework underpins IN617's remarkable high-temperature strength, creep resistance, and oxidation resistance, making it highly suitable for demanding applications in advanced power plants and gas turbine engines [9] [2].

2.3 Precipitates Formed in IN617 and Their Microstructure

During high-temperature aging of IN617 superalloy, the primary precipitates observed are $M_{23}C_6$ carbides, the γ' (gamma prime) phase, and a minor amount of MC carbides.

2.3.1 M23C6 Phase

These carbides (where M = Cr, Mo, etc.) preferentially precipitate along grain boundaries and, as this study reveals, especially at twin boundaries. In the microstructure, $M_{23}C_6$ carbides appear as thin, continuous films or discrete particles decorating the grain and twin boundaries. Their precipitation is driven by the selective diffusion of chromium and molybdenum to these high-energy interfaces. Over time, these carbides can coarsen, but the presence of adjacent γ' phase can inhibit this coarsening, helping to stabilize the microstructure.

(a): Shows a high-magnification microstructure with MX carbonitrides, $M_{23}C_6$ carbides, and μ phase particles distributed along the grain boundary, indicating the presence of multiple secondary phases at boundaries.

(b): Displays a lower-magnification view where a large $M_{23}C_6$ carbide and an adjacent MX particle are present within the grain interior, highlighting the formation of coarse precipitates away from grain boundaries.

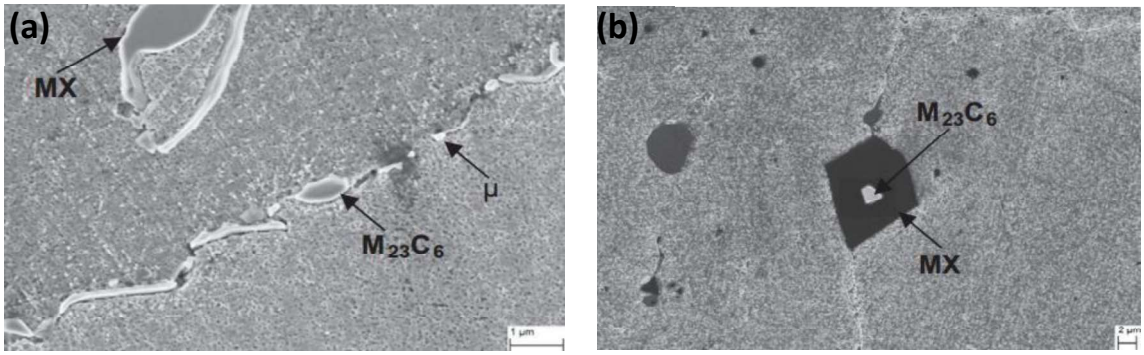

Fig. 2.1: SEM image of a mix of MX, M_6C and $M_{23}C_6$ precipitates at GB [4].

2.3.2 γ' (Gamma Prime) Phase: The γ' phase (Ni_3 (Al, Ti)) is the key strengthening precipitate in IN617, possessing an ordered $L1_2$ crystal structure. In this study, γ' is found to nucleate preferentially at the interface between twin boundaries and $M_{23}C_6$ carbides, forming a unique twin boundary/$M_{23}C_6$/γ' composite microstructure. The γ' phase undergoes a multi-stage evolution: starting from disordered atomic aggregation, progressing to ordered precipitation, then coarsening, and eventually partial dissolution. In micrographs, γ' typically appears as fine, cuboidal or spherical precipitates at or near the twin boundary/$M_{23}C_6$ interface [10].

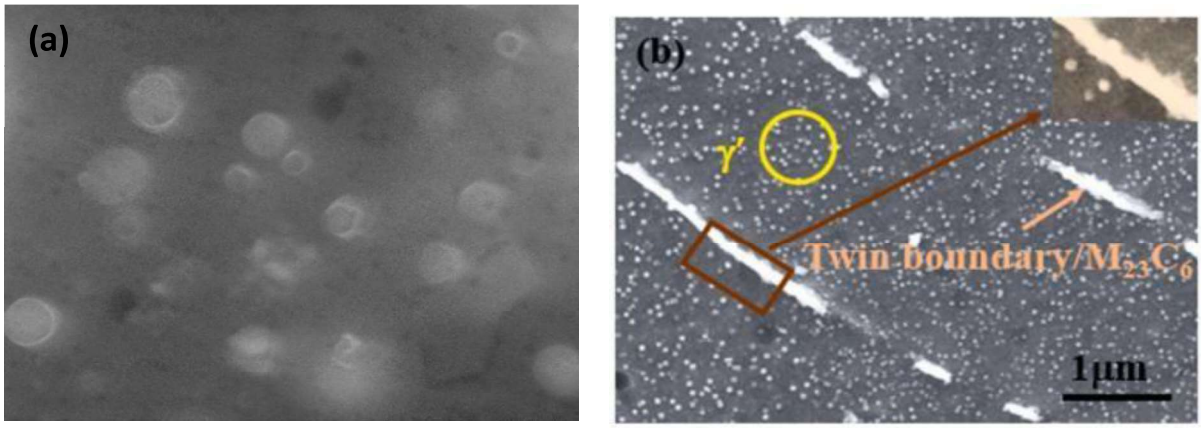

Fig. 2.2. Microstructures of the samples under different conditions: (a) aged for 5000 hr; (b) as-solution treated [4].

The presence of these particles significantly contributes to the alloy's strength by pinning dislocations, which improves both creep resistance and overall mechanical stability. Despite prolonged exposure, a substantial volume fraction of γ′ is retained, indicating its thermal stability and effectiveness in maintaining the hardness and strength of the alloy. (a): Shows a microstructure with numerous round, bright particles distributed throughout the matrix, indicating the presence of uniformly dispersed precipitates or secondary phase particles within the grains,(b): Displays a higher-magnification image highlighting a twin boundary decorated with elongated $M_{23}C_6$ carbides, while also showing γ' precipitates within the grain, demonstrating preferential precipitation of carbides along the twin boundary and fine γ' phase in the matrix. The persistence and coarsening of γ′ overtime demonstrate its vital role in ensuring that IN617 can reliably perform in demanding environments such as ultra-supercritical boiler tubes and gas turbine components.

2.3.3 M_6C Phase:

The M_6C carbide in IN617 is a molybdenum-rich phase that plays a significant role in the alloy's microstructural stability and mechanical properties during long-term high-temperature exposure. In the as-received condition, only a small amount of M_6C is present, but after 65,000 hours of operation at 800 °C, the area fraction of M_6C increases substantially, indicating its initial stability and effectiveness in strengthening the alloy. These carbides are typically found both within grains and along grain boundaries, often appearing as white, irregular, or quasi-spherical particles under SEM. (a): Shows a microstructure with multiple secondary phases including MX carbonitrides, $M_{23}C_6$ carbides, and μ (mu) phase precipitates distributed throughout the matrix, demonstrating the complex precipitation behavior during

thermal exposure,(b): Displays a grain boundary (GB) with precipitates formed along the boundary interface, indicating preferential nucleation and growth of secondary phases at grain boundaries during heat treatment .

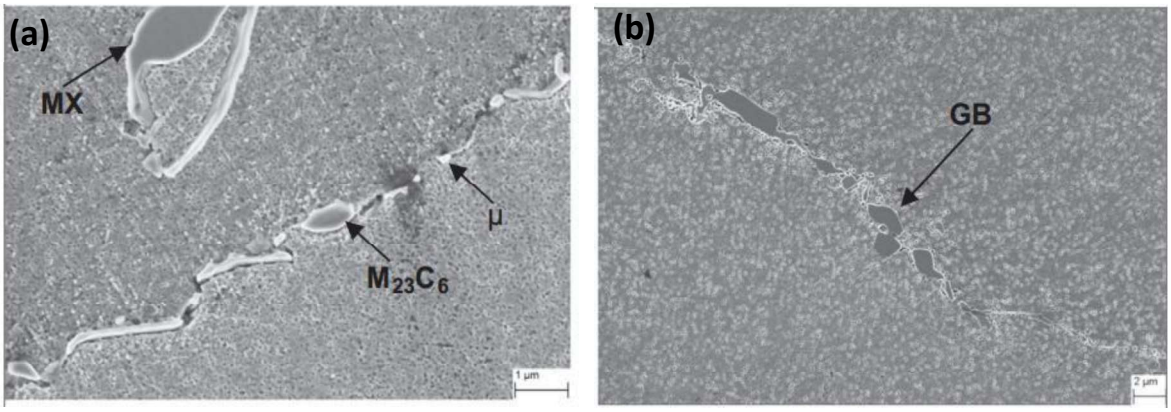

Fig.2.3 (a) $M_{23}C_6$ and μ phase at GB and intragranular MX; SEM image of a mix of MX, M_6C and $M_{23}C_6$ precipitates at GB [3].

However, with further prolonged exposure (up to 98,000 hours), the fraction of M_6C decreases due to a transformation reaction ($M_6C + \gamma \rightarrow M_{23}C_6 + \gamma'$), reflecting its partial instability over very long times. Overall, M_6C carbides contribute to the alloy's hardness and strength, especially in the early and mid-stages of service, but their reduction over time highlights the dynamic evolution of strengthening phases in IN617 during extended high- temperature operation [11].

2.4 Challenges of IN617 During Longer Exposure

During prolonged exposure at 760 °C, Inconel 617 (IN617) superalloy faces several challenges that affect its mechanical properties and microstructure. The primary issue is the precipitation of carbides (mainly $M_{23}C_6$ and M_6C) and γ′ phase particles. Initially, carbides form both within the grains and along grain boundaries, with the γ′ phase remaining intragranular. After 3,000 hours of aging, carbides at grain boundaries are discontinuous, but by 5,000 hours, they merge and form continuous networks. This continuous precipitation at grain boundaries significantly weakens the boundary strength, leading to a marked reduction in toughness, especially after the first 300 hours of aging. The fracture mode of the alloy shifts from ductile to brittle due to the formation of these carbides, as cracks tend to initiate and propagate along the weakened grain boundaries [12].

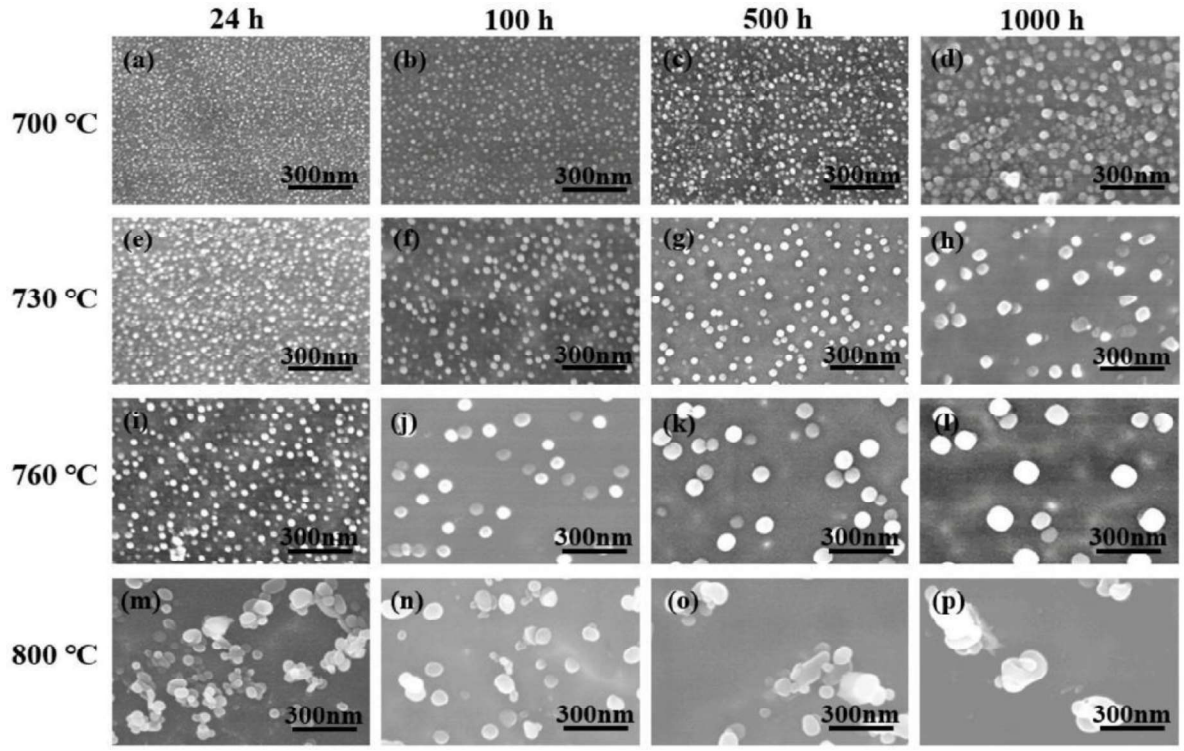

Fig.2.4 Evolution of the γ′ phase in IN617 alloy after aging at 700–800 ◦C for 24, 100, 500, and 1000 h, respectively: (a–d) 700 ◦C; (e–h) 730 ◦C; (i–l) 760 ◦C; (m–p) 800 ◦. [6].

The hardness of IN617 increases notably during the early stages of aging (up to 3,000 hours), primarily due to the precipitation of carbides and some γ′ phase, which act as barriers to dislocation motion. However, after 5,000 hours, hardness decreases, likely because of increased M_6C carbides and reduced Mo solution strengthening. The ductility of the alloy drops sharply after the initial 300 hours of aging and then remains relatively stable at a lower level. Despite these changes, the high-temperature tensile strength of IN617 remains stable between 300 and 3,000 hours of aging. Importantly, the size and volume fraction of intragranular carbides and γ′ phase do not change significantly even after 10,000 hours, indicating good microstructural stability within grains. However, the continuous precipitation of carbides at grain boundaries dominates the degradation of mechanical properties during long-term exposure, making intergranular fracture and reduced toughness the most critical challenges for IN617 in prolonged high-temperature service [13].

"Summary of Studies of Aging and Environmental Effects on Inconel 617 and the major challenges faced by IN617 during long-term exposure at high temperatures are primarily related to environmental degradation and microstructural changes. The alloy is exposed to

helium coolant containing impurities such as water vapor and carbon monoxide, which can lead to oxidation, carburization, or decarburization depending on their concentration and temperature. The stability of the protective chromium oxide (Cr_2O_3) scale is essential for corrosion resistance, but deviations in coolant chemistry can compromise this layer, accelerating material loss and reducing component life. Prolonged high-temperature exposure also results in the formation of a carbide-depleted zone beneath the oxide scale and causes grain growth, broadening the distribution of grain sizes.

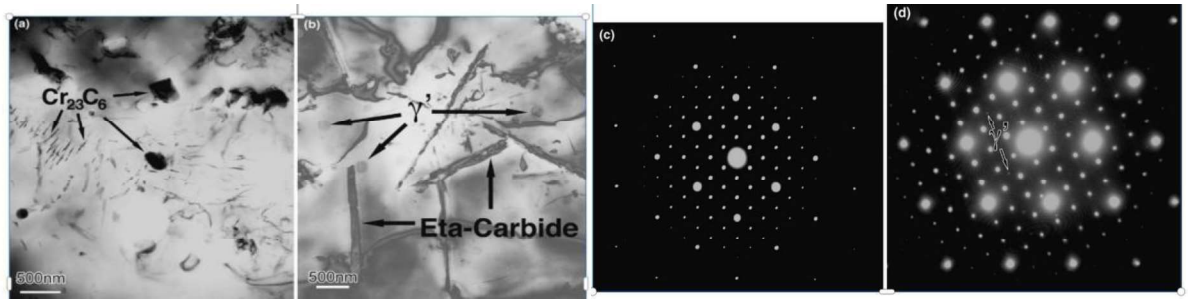

Fig 2.5 Sample 04, aged at 704 C for 43,100 h. (a) BF image of coarse $M_{23}C_6$ carbide with c¢ precipitates around and (b) corresponding [011] $M_{23}C_6$ // [011] matrix SAD pattern showing reflections from twinned carbides and c¢ precipitates; (c) BF image showing fine M23C6 carbides and dislocations in the matrix, and (d) corresponding [011] $M_{23}C_6$ // [011] matrix SAD pattern[8].

These microstructural changes are associated with a gradual decrease in yield strength, as larger grains typically reduce mechanical strength. Additionally, aging underload can lead to the redistribution of carbides to grain boundaries, especially at certain temperatures and stress levels, which weakens these boundaries and increases the risk of intergranular fracture. Although the mechanical property changes are generally modest, the combined effects of environmental attack, grain growth, carbide redistribution, and decreased yield strength present significant challenges for the long-term reliability of IN617 in demanding applications such as next-generation nuclear plant heat exchangers.

These factors must be carefully managed to ensure the safe, efficient, and durable operation of IN617 components in high-temperature environments [2]. (a): Shows a TEM microstructure with dark $Cr_{23}C_6$ carbide precipitates distributed throughout the matrix, indicating the formation of chromium-rich carbides during thermal exposure at 500nm scale,

(b): Displays a TEM image revealing γ' precipitates and Eta-Carbide phase, with arrows indicating the location of these secondary phases within the microstructure at 500nm magnification. And (c): Presents a selected area electron diffraction (SAED) pattern showing

discrete diffraction spots on a dark background, indicating the crystalline nature of the examined region, and (d): Shows a more complex SAED pattern with additional diffraction spots and indexing markers, suggesting the presence of multiple phases or orientations within the selected area.

In summary, the major challenges for IN617 during long-term high-temperature exposure include environmental degradation from oxidation, carburization, and decarburization due to impurities in helium coolant. The stability of the protective Cr_2O_3 oxide layer is critical but can be compromised by changes in gas chemistry. Prolonged aging also leads to grain growth and the formation of a carbide-depleted zone, reducing yield strength. Additionally, carbides tend to redistribute to grain boundaries under load, increasing susceptibility to intergranular fracture. These combined effects threaten the alloy's long- term mechanical integrity and reliability in demanding reactor environments.

2.5 Mechanical Property Degradation and Creep Behaviour

The mechanical properties of Inconel 617 (IN617) under long-term high-temperature exposure have been a focus of extensive research due to its critical role in next-generation nuclear plant heat exchangers. According to the INL/EXT-06-11750 report, IN617 demonstrates a high level of creep resistance, which is essential for maintaining structural integrity at reactor outlet temperatures approaching 950–1000°C.

However, prolonged exposure to these elevated temperatures leads to notable microstructural changes, including the formation of an adherent oxide scale and a carbide-depleted zone beneath the oxide. These changes are accompanied by some grain growth and a broader distribution of grain sizes, both of which are linked to a gradual decrease in yield strength over time. Mechanical testing, as summarized in the report, shows that the reduction in yield strength is consistent with the observed increase in grain size during aging. Additionally, aging under applied load causes a redistribution of carbides, with a tendency for carbides to migrate to grain boundaries that experience tensile stresses.[14] This redistribution can weaken grain boundaries, making the alloy more susceptible to intergranular fracture, especially under creep conditions. Despite these changes, the report notes that the overall degradation in mechanical properties is modest for the aging conditions studied, with IN617 retaining a significant portion of its strength and ductility even after thousands of hours at high temperature. Creep tests conducted under various conditions confirm that IN617 maintains superior creep resistance compared to many alternative alloys, which is a primary reason for its selection in demanding reactor environments. Nevertheless, the combined effects of microstructural evolution-such as grain growth, carbide depletion, and carbide redistribution-necessitate careful consideration in design and lifetime assessment, as they can influence long-term mechanical stability and the onset of creep-related failures [15]. Overall, while IN617 remains a leading candidate for high-temperature applications, ongoing studies emphasize the importance of monitoring and understanding its mechanical property degradation mechanisms to ensure safe and reliable operation over extended service periods.

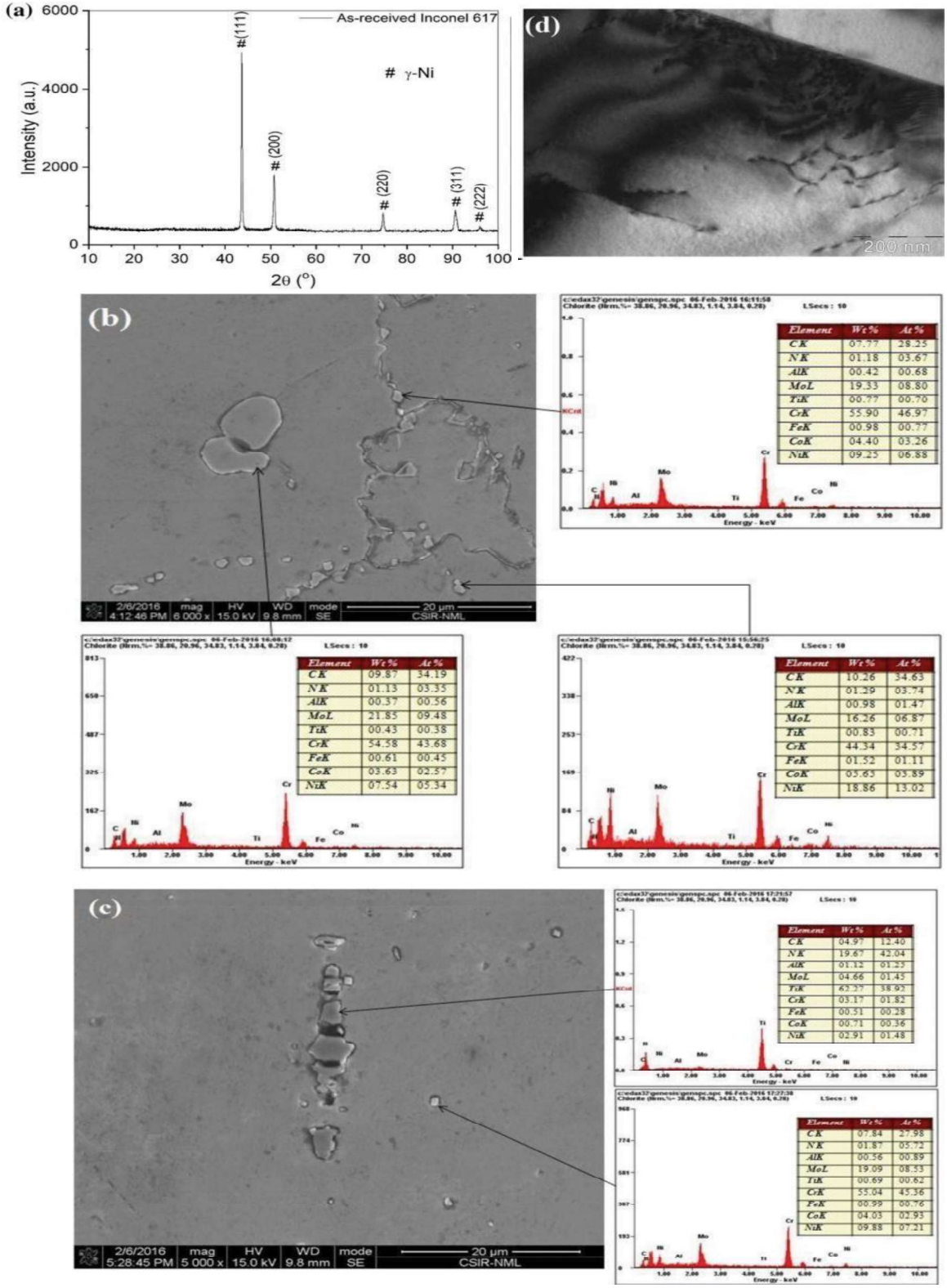

Fig.2.6 Pre-creep microstructure of the as-received IN617 alloy: (a) XRD pattern of as-received IN617 alloy showing the peaks of c-Ni phase, (b and c) SEM (SE) images depicting the presence of intergranular and trans granular (Cr, Mo)$_{23}$C$_6$ precipitates and trans granular Ti(C,N) precipitates; as well as (d) TEM images at higher magnification (compared to (b) and (c)) revealing the absence of c¢ precipitates [15].

The mechanical properties and creep behavior of INCONEL 617 (IN617) under long-term high-temperature exposure are crucial for its use in ultra-supercritical (USC) power plant applications, where service temperatures can reach 750 °C and high pressures are sustained for tens of thousands of hours. This study investigates IN617 specimens subjected to creep at 650–750 °C for up to 20,000 hours, focusing on microstructural evolution and its link to mechanical performance. The results show that IN617 maintains a stable grain structure during prolonged creep, with average grain sizes remaining relatively consistent and no significant grain degeneration or cavitation observed. The alloy's hardness decreases moderately after long-term exposure, reflecting changes in precipitate distribution and potential softening due to microstructural evolution. Microstructural analysis reveals that the main precipitates present in both as-received and crept samples are $M_{23}C_6$ carbides and MX-type particles, with additional μ phase forming only at temperatures above 700 ° C. The size, volume fraction, and inter-particle spacing of these precipitates vary depending on the thermal and mechanical history, directly influencing creep resistance. The presence of finely dispersed γ' and carbides contributes to the alloy's hardening and impedes dislocation motion, which is essential for maintaining creep strength. However, over time, coarsening of precipitates and changes in their distribution can reduce their effectiveness as barriers to deformation, leading to a gradual decrease in hardness and creep strength. Despite these changes, IN617 demonstrates excellent microstructural stability and resistance to creep rupture, meeting the demanding requirements for high-temperature applications. The study also employs a continuum damage mechanics (CDM) model, validated by experimental data, to predict the long-term creep behaviours of the alloy based on quantitative microstructural parameters. Overall, while some degradation in mechanical properties occurs due to precipitate evolution and slight grain growth, IN617 retains a high level of creep resistance and structural integrity, confirming its suitability for advanced power generation systems operating under extreme conditions.[14][15]. In conclusion, the long-term mechanical performance of IN617 is governed by a complex interplay between microstructural evolution and environmental exposure at elevated temperatures. Both literature sources confirm that while IN617 exhibits excellent creep resistance and retains much of its structural integrity after thousands of hours at high temperature, gradual changes such as grain growth, carbide coarsening, and redistribution of precipitates can lead to moderate reductions in hardness and yield strength.

The stability of the grain structure and the presence of finely dispersed carbides and γ' phase are critical factors in maintaining creep strength, but their evolution over time- particularly the migration of carbides to grain boundaries- can increase susceptibility to intergranular fracture. [3] Despite these degradative trends, IN617 remains a leading candidate for high temperature applications due to its superior combination of creep resistance and microstructural stability. Continued research and modelling efforts are essential to accurately predict long-term behavior and ensure the safe, reliable use of IN617 in advanced power generation.

The as-received (AR) IN617 sample in this study was not subjected to creep testing, and therefore no hardness value is reported for this condition. After prolonged creep exposure at temperatures ranging from 650°C to 750°C for up to approximately 20,000 hours, IN617 demonstrated a relatively stable grain size, with only moderate changes observed among the different test specimens. Hardness measurements indicated a slight decrease with increasing temperature and exposure time, reflecting some softening of the alloy as a result of microstructural evolution. These findings underscore the alloy's robust microstructural stability and its resistance to significant mechanical property degradation during extended high-temperature service. Overall, the results confirm that IN617 maintains much of its mechanical integrity under demanding conditions, supporting its suitability for long-term, high-temperature applications.

Table 2.1: Average Grain Size and Hardness of IN617 Specimens After Long-Term Creep Exposure [16].

Sample	Creep Temperature (°C)	Load (MPa)	Time (hrs)	Average Grain Size (µm)	Hardness (HV)
As Received	-	-	-	156 ± 36	-
1	650	130	19,299	137 ± 38	365 ± 18
2	700	110	20,764	123 ± 31	322 ± 23
3	00	94	20,168	176 ± 29	343 ± 19
4	750	68	16,075	148 ± 28	331 ± 21

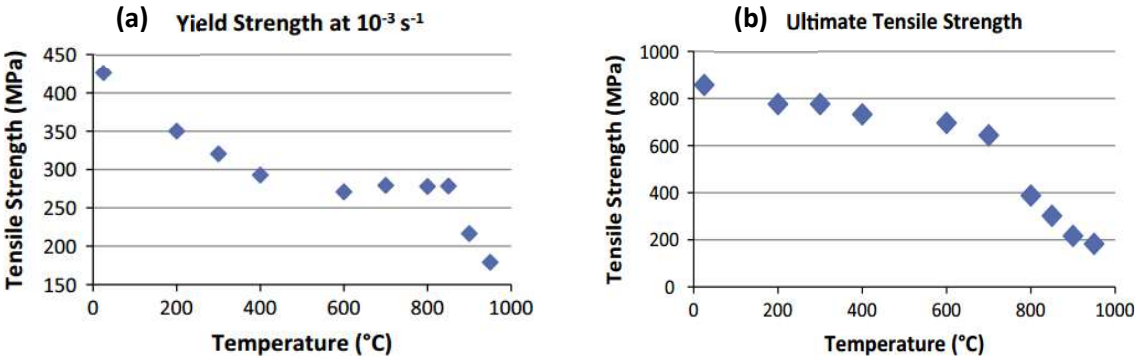

Fig.2.7. Mechanical properties of Inconel 617 and Haynes 230 as a function of temperature at a strain rate of 103 s1 showing (a) yield strength, (b) ultimate tensile strength, and (c) total elongation [16].

In this graph (a): Shows yield strength decreasing from ~430 MPa at room temperature to ~180 MPa at 1000°C, with some fluctuations in the intermediate temperature range, indicating thermal softening and loss of precipitation strengthening at elevated temperatures. And in (b): Displays ultimate tensile strength declining from ~870 MPa at room temperature to ~190 MPa at 1000°C, showing a more gradual decrease initially followed by a steeper drop above 600°C, reflecting the progressive loss of strengthening mechanisms with increasing temperature.

Chapter 3

Experimental Methodology

3.1 Sample preparation

Nine samples of different thermal history conditions were prepared for comprehensive microstructural characterization. The samples included an as-received (solution zed) specimen and eight thermally aged specimens at various temperatures (650°C, 700°C, 750°C, and 800°C) and durations (120-5000hrs). All specimens were sectioned to dimensions of approximately 10×10×5 mm using a precision cutting machine with diamond-embedded blade under constant cooling to prevent microstructural alteration. A systematic metallographic preparation procedure was employed involving sequential grinding and polishing steps. Initially, all samples were ground using silicon carbide (Sic) abrasive papers of increasing grit numbers (240, 400, 600, 800, 1000, and 1200) under constant water cooling. Each grinding step was performed for 3-5 minutes with the sample rotated 90° between successive steps to eliminate directional scratches. Following grinding, specimens were polished using diamond suspensions of decreasing particle sizes (6μm, 3μm, and 1μm) on separate polishing cloths. Final polishing was achieved using 0.05μm colloidal silica suspension for 10 minutes to obtain a mirror-like, scratch-free surface. Between each polishing step, samples were ultrasonically cleaned in ethanol for 5 minutes to remove any residual abrasive particles and dried using compressed air.

. For optical microscopy, selected samples were etched using an appropriate etchant Aqua regia 1:3(HCl: HNO_3) to reveal microstructural features. The etched specimens were examined using an optical microscope at magnifications ranging from 50× to 1000×.

a. As received sample (solution zed).

b. Aged at 650°C for 120 Hrs.

c. Aged at 700°C for 5000 Hrs.

d. Aged at 700°C for 1000 Hrs.

e. Aged at 750°C for 120 Hrs.

f. Aged at 800°C for 120 Hrs.

g. Aged at 700 °C for 120 Hrs.

h. Aged at 700 °C for 3000Hrs.

i. Aged at 700 °C for 500 Hrs.

3.2 Experimental Methodology for Precipitate Extraction and Analysis

3.2.1 Selection and Identification of Samples

Industrial Relevance: Samples were sourced from BHEL to ensure that the material reflects actual industrial production standards and quality, making the study outcomes directly applicable to real-world engineering applications.

Material Uniformity: The supplied samples were verified to be from the same production batch, ensuring uniformity in chemical composition and processing history. This minimizes variability and enhances the reliability of comparative analysis.

Representative Size and Form: The samples were provided in dimensions suitable for all planned metallographic, mechanical, and extraction analyses, ensuring that each specimen was large enough for repeated testing and characterization.

Availability of Thermal History: The selection included both as-received (solutionzed) and thermally aged specimens, covering a range of service-relevant conditions.

3.2.2 Initial Mass Measurement

- All 8 IN617 samples (as-received + 7 thermally aged at 650°C–800°C for 120– 5000 hrs) were individually weighed using a METTLER TOLEDO XPE206 analytical balance (±0.0001 g precision).
- Initial masses ranged from 6.72 g to 8.81 g, recorded to 3 decimal places.

3.2.3. Electrolytic Extraction Setup

3.2.3.1 Current Density Calculation

Exposed surface area (A) of each sample measured using digital callipers (±0.01 mm precision). For rectangular sample. A = 2(lw +lt +wt.) cm

Where,

l=length, w=width, t=thickness

Applied current (I) calculated: I=A×0.1 A/cm2

Where, 0.1 A/cm² was empirically determined as optimal for matrix dissolution while preserving precipitates.

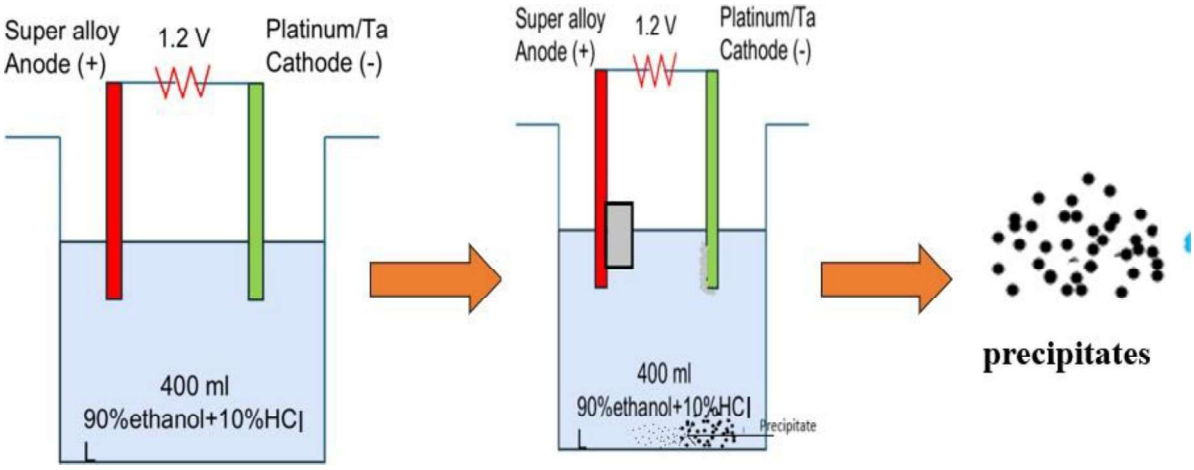

Fig3.1: Schematic representation of the electrolytic extraction process used to isolate precipitates from IN617 superalloy using a 90% ethanol + 10% HCl solution at 1.2 V.

Example: Sample with 2.5 cm² surface area received 0.25 A current.

- Each sample served as the anode in a dedicated electrolytic cell to prevent cross-contamination.
- Electrolyte: 400 mL solution of 90% ethanol + 10% HCl (vol%).
- Constant voltage: 1.2 V (Tantalum cathode).

3.2.4. Post-Extraction Processing

- Dissolved matrix was vacuum-filtered through 0.2 μm pore-size filter paper.
- Filter papers with precipitates were dried at 50°C for 24 hrs in a vacuum oven.

3.2.5. Precipitate Quantification

- Residual matrix mass: Weighed after extraction.
- Precipitate mass: Calculated as:

  mass precipitate= mass Initial- mass residual
- Repeat measurements showed <2% variation between replicates.

3.2.6. Sample Characterization

After the extraction and drying of precipitate powders from the IN617 superalloy, a comprehensive characterization was performed to determine their phase composition, morphology, and elemental distribution.

The primary techniques employed were X-ray Diffraction (XRD), Scanning Electron Microscopy (SEM), and Energy Dispersive X-ray Spectroscopy (EDS), as illustrated in Step 6 of the process flow chart.

X-ray Diffraction (XRD): XRD was used to identify and quantify the crystalline phases present in the extracted precipitates. The dried powder samples were mounted on a zero-background holder and scanned using Cu-Kα radiation over a 2θ range of 20°–100°. The resulting diffraction patterns were analysed to determine the presence of various phases such as γ, γ', carbides (e.g., MC, $M_{23}C_6$), and any other intermetallic compounds. This technique is essential for understanding the phase evolution in superalloys after different thermal exposures, as it reveals phase transformations and the stability of strengthening precipitates.

Scanning Electron Microscopy (SEM); SEM provided high-resolution imaging of the precipitate powders, allowing for detailed observation of particle morphology, size distribution, and surface features. The samples were sputter-coated with a thin layer of gold to enhance conductivity and minimize charging effects. SEM images helped to distinguish between different precipitate types based on their shape and size, such as the identification of blocky carbides or fine γ' particles. This morphological information is crucial for correlating microstructural features with mechanical properties and service performance.

Energy Dispersive X-ray Spectroscopy (EDS): EDS analysis was conducted in conjunction with SEM to determine the elemental composition of the precipitates. EDS spectrum and elemental maps provided quantitative and qualitative data on the distribution of key alloying elements (e.g., Ni, Cr, Mo, Al, Ti, C) within individual precipitate particles. This allowed for the differentiation of various carbide and intermetallic phases and the assessment of compositional homogeneity. The combination of SEM and EDS is particularly effective for analysing complex, multi-phase superalloy systems.

The comprehensive characterization of the extracted precipitates using X-ray Diffraction

(XRD), Scanning Electron Microscopy (SEM), and Energy Dispersive X-ray Spectroscopy (EDS) provided a detailed understanding of the phase composition, morphology, and elemental distribution within the IN617 superalloy. The integration of these analytical techniques enabled both qualitative and quantitative insights into nature and evolution of precipitate phases formed under various thermal conditions. This robust characterization forms the foundation for correlating microstructural features with the alloy's mechanical properties and long-term performance. The findings from this section not only validate the effectiveness of the extraction methodology but also offer critical information for optimizing alloy processing and predicting service behavior in high- temperature applications.

3.3. Flow Chart of Extraction and Analysis Process

3.3.1 Extraction and Analysis Workflow for Precipitate Characterization

The extraction and characterization of precipitates from the IN617 superalloy were performed through a systematic, multi-step methodology. Each stage was carefully designed to ensure the selective isolation of precipitate phases from the alloy matrix, followed by comprehensive qualitative and quantitative analysis. The overall workflow is summarized in Figure X (see flow chart).

3.3.2. Bulk Sample Selection

The process begins with the selection of a representative bulk sample of IN617 superalloy, as shown in Step 1 of the flow chart. These samples were sourced from Bharat Heavy Electricals Limited (BHEL), ensuring industrial relevance and uniformity in chemical composition. Each sample was visually inspected for surface defects and irregularities prior to further processing. This initial step is crucial to ensure that the extracted precipitates accurately reflect the microstructural state of the alloy under the specified thermal history.

3.3.3 Weighing

Accurate quantification of the sample mass is essential for subsequent calculations of precipitate yield and extraction efficiency. In Step 2, each bulk sample was weighed using an analytical balance with a precision of ±0.0001 g. The initial mass was recorded in a laboratory logbook for traceability. This measurement serves as the baseline for determining the mass of matrix dissolved and the mass of precipitates isolated after the extraction process.

3.3.4. Electrolysis

The core of the extraction process is the electrolytic dissolution of the alloy matrix, depicted in Step 3. The weighed sample was mounted as the anode in a custom-designed electrolytic cell, with a tantalum cathode. The electrolyte consisted of a solution of 90% ethanol and 10% hydrochloric acid (HCl), chosen for its ability to selectively dissolve the Ni-based matrix while preserving the integrity of carbide and intermetallic precipitates. A constant current was applied during electrolysis, with the current value calculated based on the exposed surface area of the sample multiplied by a factor of 0.1 A/cm².

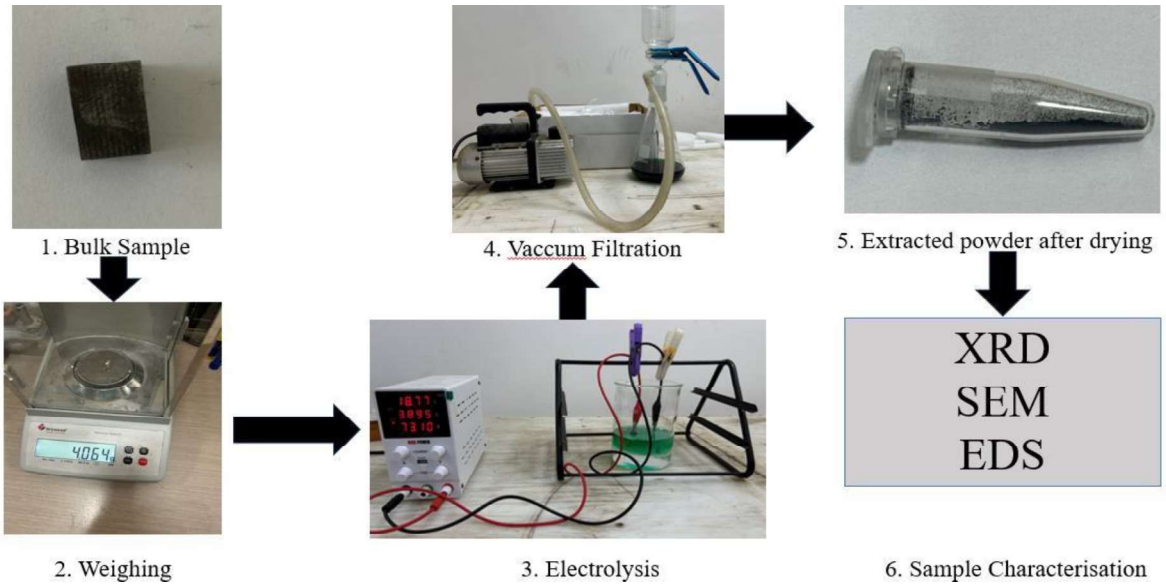

Fig3.2: Workflow for precipitate extraction and characterization from IN617 superalloy, including weighing, electrolysis, filtration, drying, and analysis by XRD, SEM, and EDS.

This current density was optimized to achieve efficient matrix dissolution without damaging the precipitates. The voltage was monitored throughout the process, typically ranging from 1.1 to 1.3 V. The duration of electrolysis was controlled, generally lasting 1-2 hrs., until a significant reduction in sample mass and visible accumulation of precipitate particles was observed.

3.3.5. Vacuum Filtration

Upon completion of electrolysis, the mixture containing dissolved matrix and suspended precipitates was subjected to vacuum filtration (Step 4). This step involved transferring the contents of the electrolytic cell to a filtration apparatus equipped with a vacuum pump and fine-pore filter paper. The vacuum accelerated the separation of solid precipitate particles

from the liquid electrolyte, ensuring efficient recovery of even the finest particles. The filter paper containing the precipitates was then carefully removed and rinsed with ethanol to eliminate any residual electrolyte.

3.3.6. Extracted Powder After Drying

The filtered precipitates were transferred to a clean container and dried at room temperature or in a low-temperature oven to remove any remaining solvent (Step 5). The resulting dry powder consisted primarily of the extracted precipitate phases, now isolated from the bulk matrix. The mass of the dried precipitate was measured to enable quantitative analysis, such as calculating the weight percentage of precipitates relative to the initial sample mass

3.3.7. Sample Characterization (XRD, SEM, EDS)

The final stage of the workflow involves comprehensive characterization of the extracted precipitates (Step 6). Multiple analytical techniques were employed:

X-ray Diffraction (XRD): Used to identify the crystalline phases present in the precipitate powder, providing information on the types of carbides and intermetallic formed during thermal exposure.

Scanning Electron Microscopy (SEM): Provided high-resolution images of precipitate morphology, size distribution, and surface features.

Energy Dispersive X-ray Spectroscopy (EDS): Enabled elemental analysis and mapping, revealing the chemical composition and homogeneity of the precipitate phases.

These complementary techniques allowed for both qualitative and quantitative assessment of the precipitates, including phase identification, size and shape analysis, and compositional profiling. The data obtained were subsequently correlated with the thermal history of each sample to understand the evolution of precipitate characteristics under different aging conditions.

This systematic workflow, from bulk sample selection to advanced characterization, ensured the reliable extraction and detailed analysis of precipitates from IN617 superalloy. The use of electrolytic extraction, combined with precise quantification and state-of-the-art analytical methods, provided robust data on the nature and evolution of precipitates, which are critical for understanding the alloy's mechanical behavior and long-term performance.

The flow chart (Figure X) serves as a visual summary of this methodology, highlighting the logical progression and integration of each experimental step.

Chapter 4

Results and Discussions

4.1 Optical Microscopy Analysis

4.1.1 As received sample (Solutionzed)

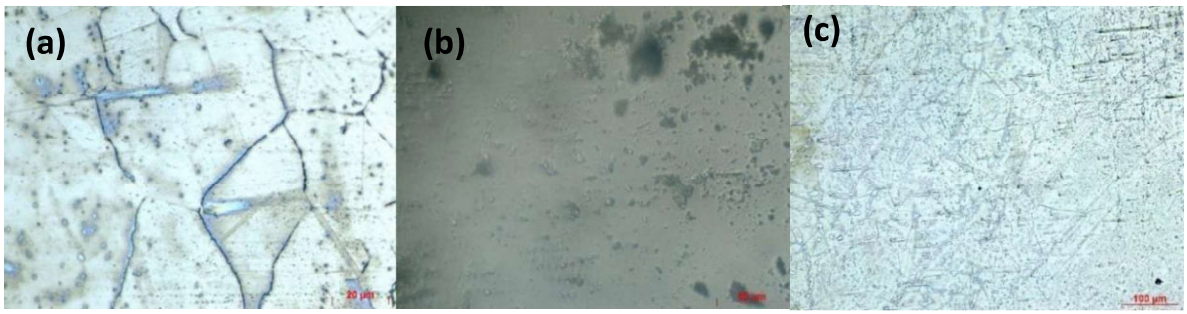

Fig 4.1.1: Optical micrographs of as-received IN617 superalloy showing equiaxed grain structure with annealing twins and dispersed primary carbides at different magnifications.

The as-received IN617 superalloy exhibits an equiaxed grain structure with well-defined grain boundaries, representing the baseline microstructure before thermal aging treatments. Fine precipitates can be observed predominantly along grain boundaries see Fig 4.1.1(a), with some intragranular precipitation also evident, characteristic of the initial carbide distribution in solution-treated nickel-based superalloys prior to age- hardening processes see Fig 4.1.1.

4.1.2 Aged at 650°C for 120 hours

The microstructure appears largely homogenous, with limited evidence of significant precipitate coarsening or elemental segregation at this aging condition. A higher density of smaller, discrete precipitates are visible within the grains compared to the grain boundaries,

suggesting a moderate degree of supersaturation see Fig4.1.2. (a): Shows large, well-defined grains with clear boundaries and minimal internal features, indicating a coarse-grained microstructure. (b): Displays smaller, more numerous grains with increased grain boundary area, suggesting grain refinement compared to (a). and (c): Reveals a highly refined microstructure with very fine grains and dense grain boundaries, typical of extensive grain refinement or recrystallization.

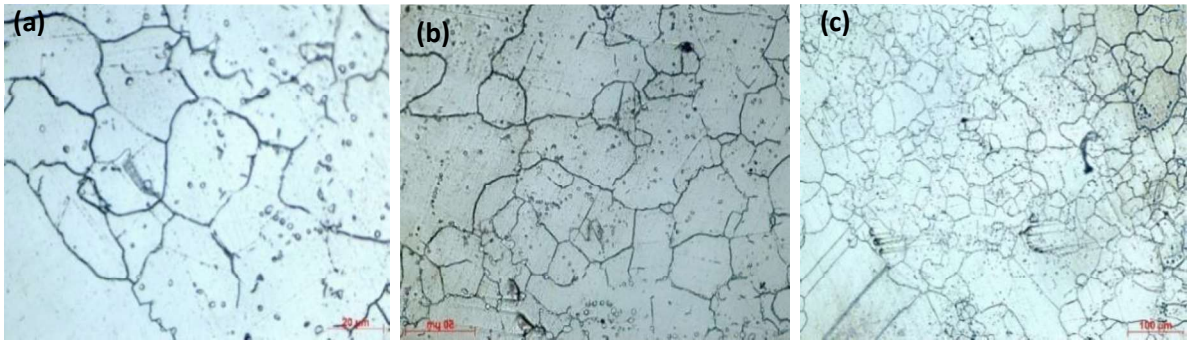

Fig4.1.2: Optical micrographs of IN617 aged at 650°C for 120 hours showing equiaxed grains with fine carbide precipitates along grain boundaries and within grains.

4.1.3 Aged at 700°C for 1000 hours

This microstructure exhibits a significant increase in grain boundary precipitation, with evidence of carbide network formation and localized elemental segregation. Fig4.1.3(a) shows a microstructure with clearly defined grain boundaries and numerous fine, evenly distributed precipitates or particles within the grains. The microstructure appears refined, with minimal grain growth and no significant voids or defects, indicating a stable, dispersion-strengthened matrix. Image (b) displays a microstructure where the grain boundaries are still visible but appear more pronounced and slightly coarser compared to (a). The presence of coarser precipitates and wider precipitate-free zones suggest diffusion-controlled growth mechanisms are active during the extended aging period

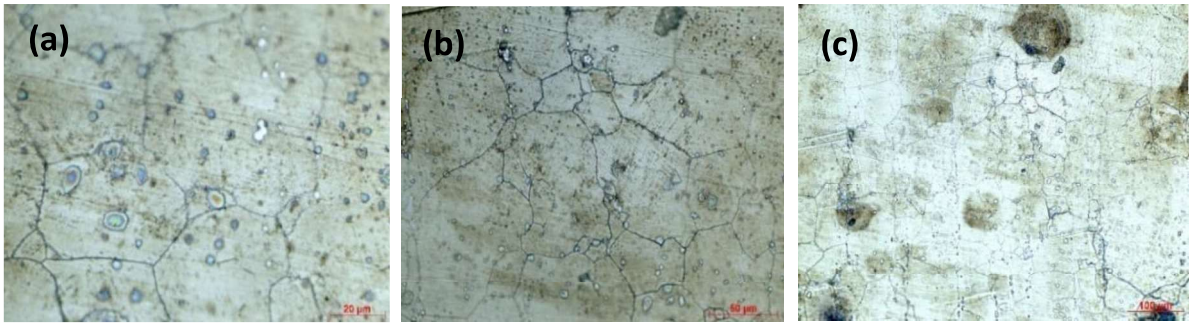

Fig4.1.3: Optical micrographs of IN617 aged at 700°C for 1000 hours revealing enhanced carbide precipitation along grain boundaries and coarsened intragranular precipitates compared to shorter aging conditions.

4.1.4. Aged at 750°C for 120 hours

The sample shows an increased density of both grain boundary and intragranular precipitates compared to above one, with a wider distribution of precipitate sizes. Fig4.1.4 (a) displays a fine-grained microstructure with well-defined grain boundaries and uniform grain size distribution. Dark precipitates are visible within grains and along grain boundaries, indicating

the presence of secondary phases or carbides. Image (b) reveals a coarser microstructure compared to (a), with larger grain sizes and more pronounced grain boundary networks, and (c): Reveals coarser grains with faint boundaries and some discoloration, typical of extensive thermal exposure and microstructural coarsening.

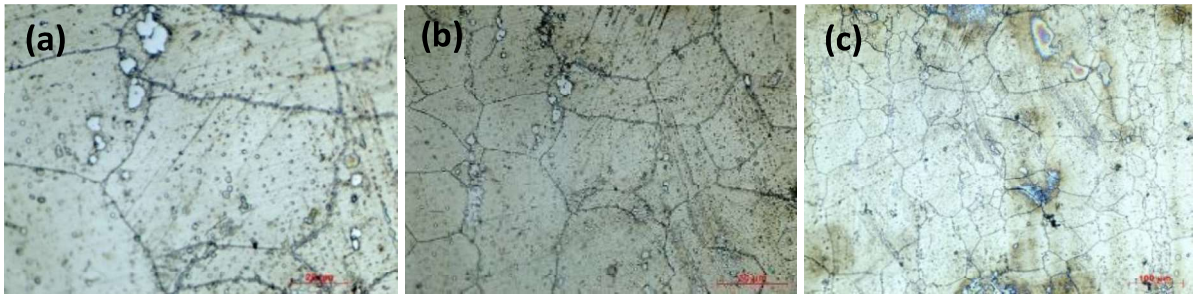

Fig4.1.4: Optical micrographs of IN617 aged at 750°C for 120 hours showing pronounced grain boundary carbides and increased intragranular precipitate density.

4.1.5 Aged at 800°C for 120 hours

In this microstructure reveals a heavily decorated grain boundary network, with extensive carbide precipitation and localized zones of substantial precipitate coarsening. The intragranular regions contain fewer, but significantly larger, precipitates, indicating the dissolution of finer particles and diffusion-driven growth of larger precipitates. The overall microstructure suggests that the alloy is approaching a more stable equilibrium state, with reduced driving force for further precipitation at this temperature. (a): Shows large, well-defined grains with clear boundaries and numerous small dark precipitates, indicating a coarse but precipitate-rich microstructure. (b): Displays moderately sized grains with visible boundaries and a slightly reduced number of precipitates, suggesting some grain refinement and precipitate coarsening. And (c): Reveals much finer grains with faint boundaries and a more uniform distribution of small precipitates, typical of significant grain refinement and advanced thermal treatment.

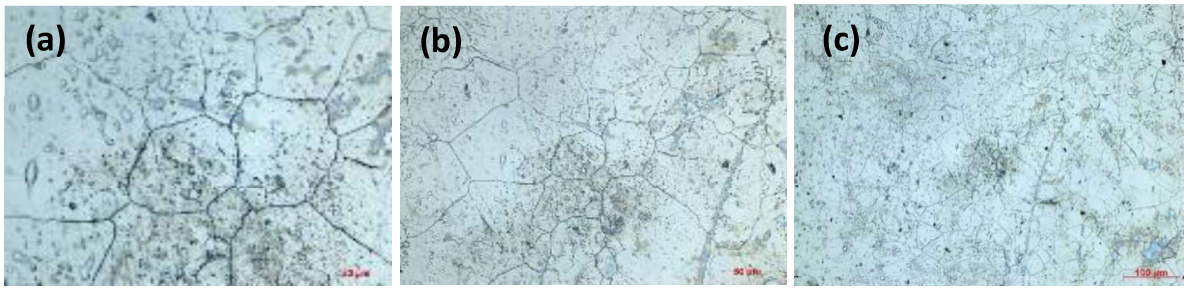

Fig4.1.5: Optical micrographs of IN617 aged at 800°C for 120 hours showing coarsened grain boundary and intragranular carbide precipitates

4.1.6 Aged at 700°C for 5000 hours

The extended aging period at 700°C has resulted in evident grain boundary decoration and the formation of larger, more pronounced precipitates, signifying substantial precipitate coarsening. There is also a non-uniform distribution of precipitates along grain boundaries, hinting at localized segregation and preferential precipitation sites, characteristic of prolonged thermal exposure. (a): Shows large, well-defined grains with clear boundaries and a few small dark precipitates, indicating a coarse-grained microstructure with minimal internal features. And (b): Displays similar large grains but with slightly more visible dark precipitates, suggesting the onset of secondary phase formation or impurity segregation along grain boundaries.

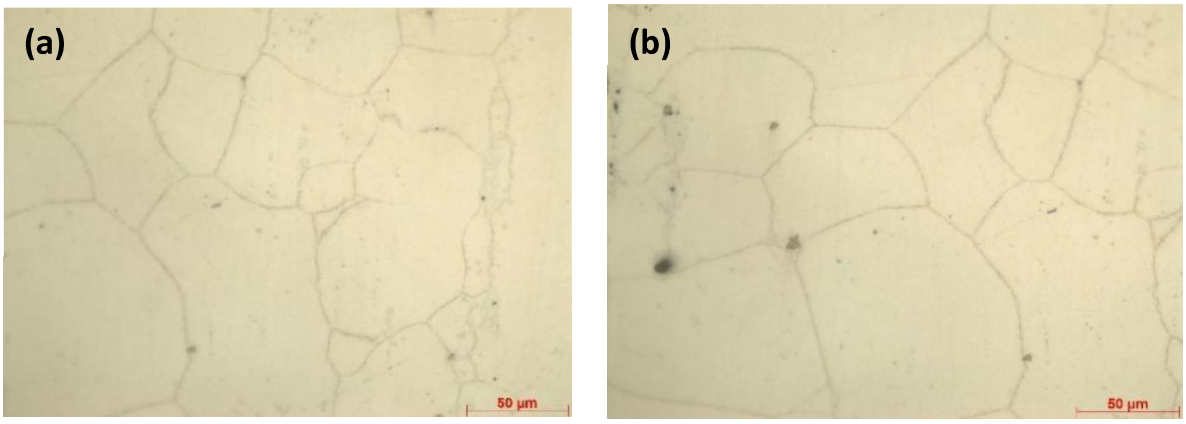

Fig4.1.6: Optical micrographs of IN617 aged at 700°C for 5000 hours showing coarsened carbide precipitates along grain boundaries and within grains.

4.2 SEM Imaging of Samples

4.2.1 As received sample (Solutionized)

The SEM images of the as-received IN617 superalloy reveal a clean matrix with a relatively uniform distribution of fine precipitates. At lower magnification (1000x) see Fig4.2.1(a), the microstructure appears free from significant defects, with only a few scattered second- phase particles and minimal evidence of carbide networks or grain boundary decoration. Higher magnification (10,000x) sees fig Fig4.2.1(c) clearly shows small, well-dispersed precipitates, likely primary carbides or nitrides, embedded within the matrix. The precipitate size is generally submicron, and their morphology appears rounded or angular, typical of carbides formed during solidification or initial processing. There is no indication of significant

coarsening, agglomeration, or elemental segregation, which suggests the alloy is in a stable, solution- treated state.

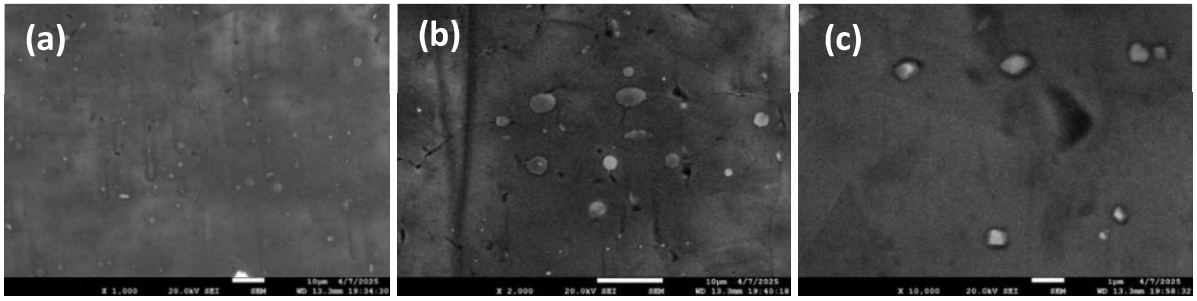

Fig4.2.1: SEM micrographs of as-received (solutionized) IN617 showing sparse distribution of primary carbides within the gamma matrix at different magnifications.

The absence of microcracks, voids, or oxidation products further confirms the integrity of the as-received sample. Overall, these features indicate a homogeneous microstructure, providing a suitable baseline for comparison with thermally aged samples.

4.2.2. Aged at 700°C for 5000 hours

The SEM images of the IN617 sample aged at 700°C for 5000 hours reveal significant microstructural evolution compared to shorter aging times. The high magnification images show considerable coarsening of γ' precipitates, see Fig4.2.2© with a distinct core-shell morphology evident in many particles, suggesting compositional changes over the extended aging period. The SEM analysis of IN617 superalloy aged at 700°C for 5000 hours reveals significant microstructural degradation driven by prolonged thermal exposure. The microstructure exhibits extensive coarsening of $M_{23}C_6$ carbides along grain boundaries, forming continuous networks with particle sizes exceeding 500 nm, which compromise grain boundary integrity.

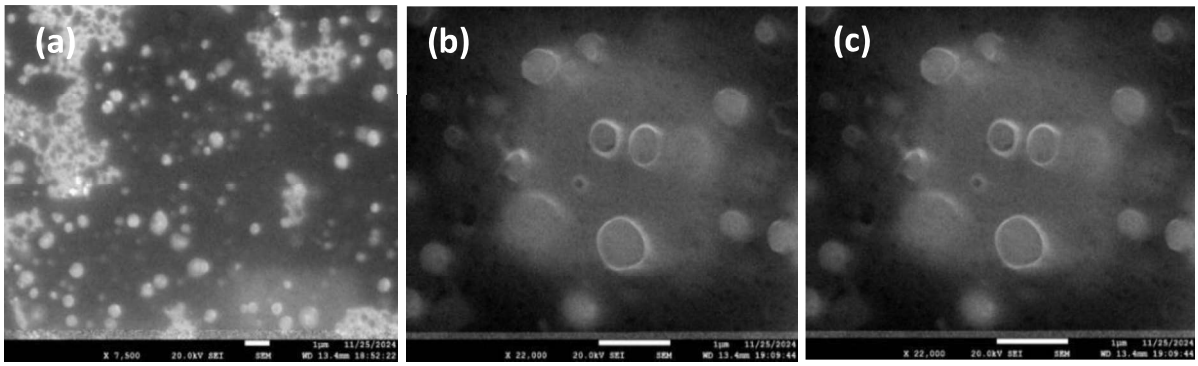

Fig4.2.2: SEM images showing extracted precipitates from IN617, highlighting spherical morphology and varying particle sizes at different magnifications.

These microstructural changes collectively correlate with reduced creep resistance, increased hardness variability, and heightened susceptibility to intergranular cracking, underscoring the alloy's performance limits under long-term high-temperature service. The observed interconnected network of γ' precipitates also implies a reduction in matrix coherency, potentially impacting the alloy's creep resistance.

4.2.3. Aged at 650°C for 120 hours

The SEM images of IN617 aged at 650°C for 120 hours see Fig4.2.3 reveal distinct microstructural changes compared to the as-received condition. Lower magnification (500x) fig Fig4.2.3(a) shows clear grain boundary precipitation, with carbides forming semi-continuous networks along grain boundaries. Higher magnification (2000x) sees fig Fig4.2.3 (c) reveals both intergranular and intragranular precipitates with varying sizes and morphologies.

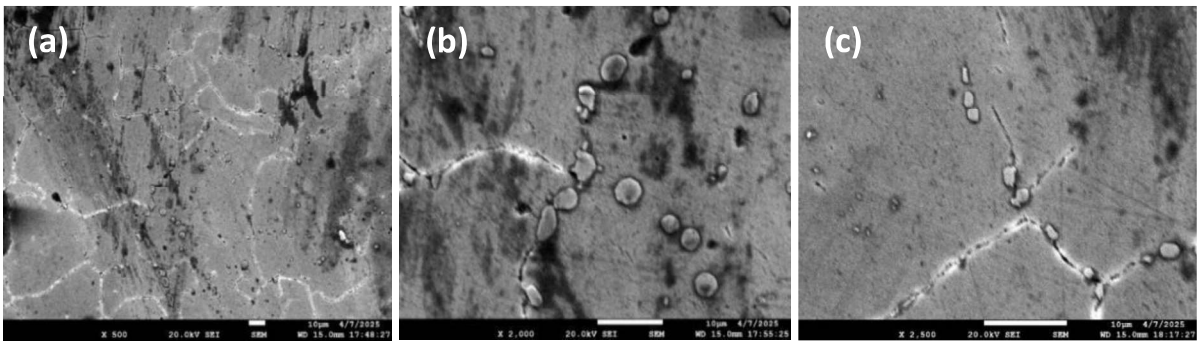

Fig4.2.3 SEM micrographs of IN617 aged at 650°C for 120 hours showing initial carbide precipitation along grain boundaries and early-stage formation of intragranular precipitates.

The intergranular carbides tend to be larger and more elongated, while the intragranular precipitates are smaller and more spherical. There is no significant evidence of extensive precipitate coarsening or the formation of large, interconnected networks, suggesting that the initial stages of precipitation are still dominant at this ageing condition. The precipitates appear relatively uniformly distributed, with some localized clustering near grain boundaries. Overall, the microstructure indicates a moderate level of thermal aging, with limited microstructural degradation.

4.2.4. Aged at 700°C for 1000 hours

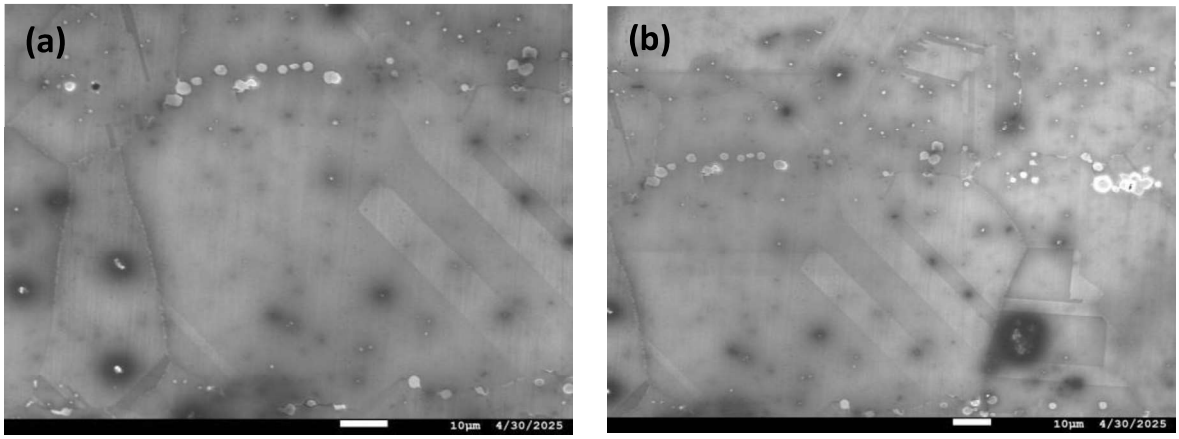

Fig4.2.4: Optical micrographs of IN617 aged at 700°C for 1000 hours showing continuous networks of M23C6 carbides along grain boundaries and increased precipitation within grains.

The SEM micrographs reveal a microstructure characteristic of a sample aged at 700°C for 1000 hours. The images display distinctive features consistent with thermal aging at this temperature-time combination. Most notably, the microstructure shows clear evidence of precipitation along what appear to be grain boundaries, shown in Fig4.2.4(a) visible as chains of bright white particles forming semi-continuous networks. These precipitates likely correspond to $M_{23}C_6$ carbides and σ phase, which typically form at grain boundaries during prolonged aging at 700°C. The 700°C aging temperature is particularly significant as it represents a condition where microstructural changes occur with heightened dynamics compared to lower temperatures. After 1000 hours at this temperature, the precipitate morphology has developed into relatively coarse and discrete particles, as clearly visible in the images. The distribution pattern of these precipitates, particularly their alignment along what appears to be grain boundaries, is consistent with the development of Cr-depleted zones that widen with increased aging time at 700°C.The microstructure also exhibits subtle contrast variations across different regions, suggesting possible variations in crystallographic orientation or composition resulting from the aging process. These features align with documented microstructural evolution in heat-resistant alloys aged at 700°C, where significant changes in precipitation characteristics and matrix composition occur after 1000 hours. The observed microstructure would be expected to correspond with modified mechanical properties, including increased strength and reduced ductility compared to the solution-annealed condition see Fig4.2.4(b).

4.3 EDS Analysis

4.3.1 As received sample

The EDS analysis of the bulk IN617 alloy reveals notable compositional variations across different regions of the material. Spectrum 1 shown Fig4.3.1(a) shows a significant presence of nickel (36.6 wt.%) and chromium (35.5 wt.%) with substantial molybdenum content (12.3 wt.%), suggesting analysis of a region rich in the γ-matrix phase with possible chromium enrichment. The ratio of these primary elements, along with the cobalt (8.4 wt.%) and carbon (5.0 wt.%) content, indicates the typical solid solution strengthened microstructure expected in IN617.

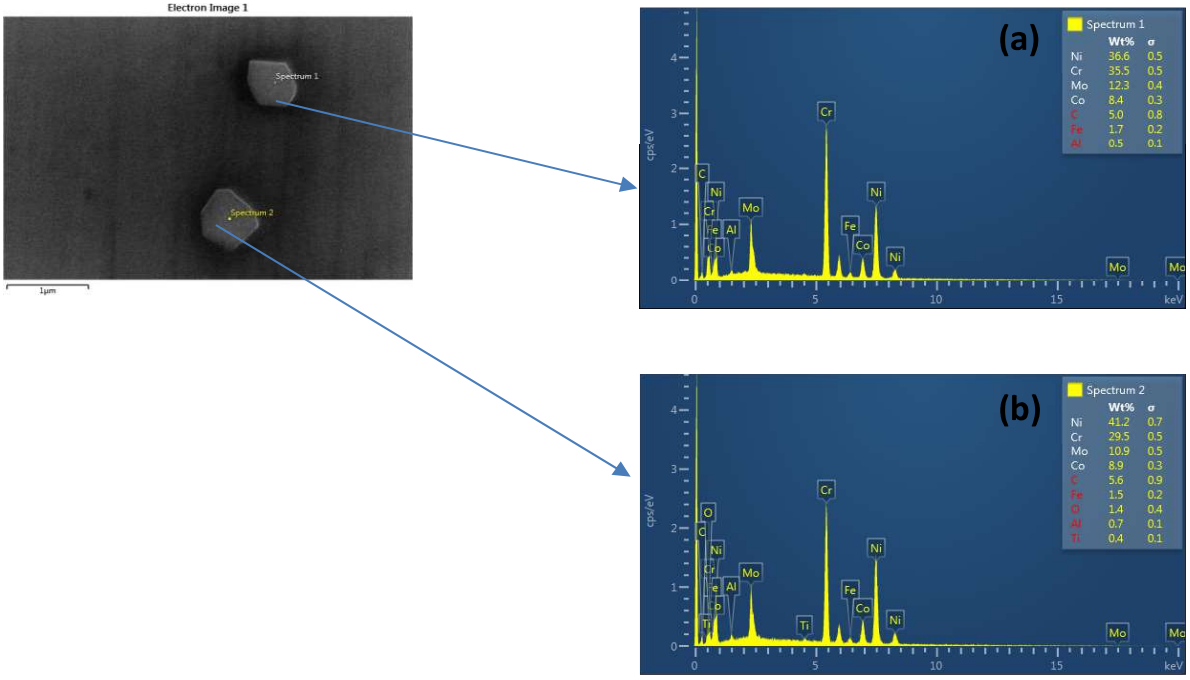

Fig 4.3.1: SEM image and EDS spectra of as-received IN617 showing isolated primary carbides with corresponding elemental compositions.

Spectrum 2 displays a higher nickel concentration (41.2 wt.%) with relatively lower chromium (29.5 wt.%), while also containing trace amounts of oxygen (1.4 wt.%) and titanium (0.4 wt.%) not detected in Spectrum 1. The detection of titanium in Spectrum 2, Albeit in small quantities, is significant as it suggests potential γ' phase nucleation sites or areas where Ti-rich MC carbides may form during subsequent thermal exposure Fig4.3.1(b). The compositional heterogeneity observed between these two spectra demonstrates the intrinsic microstructural complexity of the bulk alloy, with localized variations that will influence precipitation behavior, phase stability, and ultimately the mechanical properties

during high-temperature service. These findings provide a critical baseline for understanding the subsequent (a): Spectrum 1 shows a particle rich in Ni (36.6%), Cr (35.5%), and Mo (12.3%), with notable amounts of Co, C, Fe, and minor Al, suggesting a complex carbide or intermetallic phase with high Cr and Mo content. And (b): Spectrum 2 reveals a particle with higher Ni (41.2%) and slightly lower Cr (29.5%) and Mo (10.9%), along with Co, C, Fe, O, Al, and Ti, indicating a similar phase but with increased Ni and the presence of oxygen and titanium, possibly reflecting slight compositional variation or surface oxidation. Microstructural evolution of IN617 under various thermal conditions.

4.3.2 Aged at 700°C for 5000 hours

The EDS layered and elemental mapping images provide a comprehensive understanding of the elemental distribution within the bulk IN617 alloy. The layered EDS images clearly show that elements such as chromium (Cr), molybdenum (Mo), and iron (Fe) are preferentially enriched along the grain boundaries, as indicated by the brighter and more intense signals tracing the grain boundary network in both low and high magnification maps shown in Fig4.3.3(a).

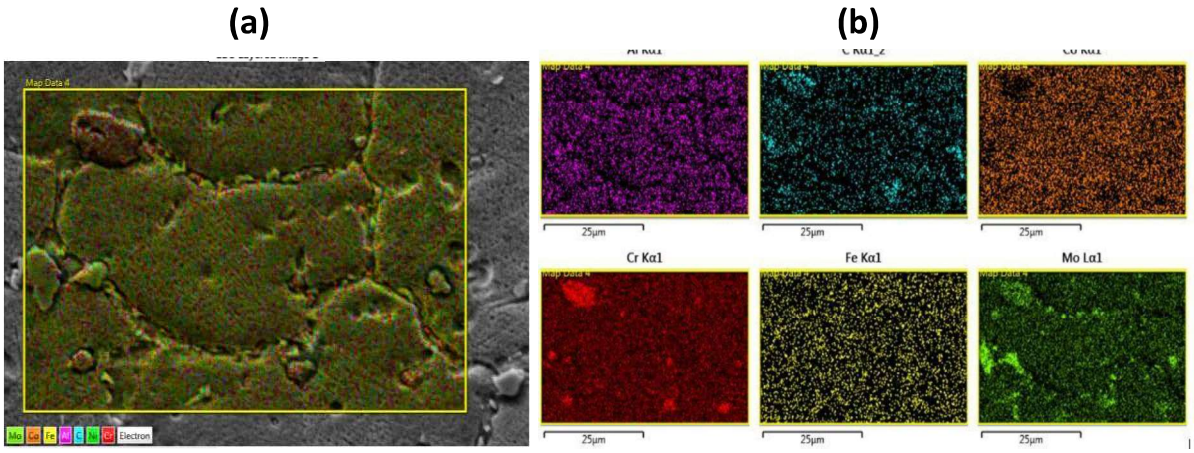

Fig4.3.2: SEM micrograph with corresponding EDS elemental distribution maps of IN617 aged at 700°C for 5000 hours showing preferential segregation of Cr, Mo, and Ti at grain boundaries and precipitates.

The individual elemental maps further confirm this observation, with Cr and Mo displaying localized concentrations at the boundaries, while elements like nickel (Ni), cobalt (Co), and aluminum (Al) are distributed more uniformly throughout the matrix, reflecting the homogeneous nature of the γ-matrix phase24. The presence of carbon (C) in the same regions as Cr and Mo suggests the formation of carbides, likely $M_{23}C_6$ or M_6C types, which are known to precipitate at grain boundaries in Ni-based superalloys and play a crucial role in enhancing

high-temperature strength and creep resistance. Notably, the higher-magnification EDS layered image highlights discrete, elongated features rich in Mo and Cr, (a): Shows an SEM image with an EDS elemental map overlay, revealing the distribution of key elements (Mo, Co, Fe, Al, Ni, Cr) across the microstructure, indicating a generally uniform but slightly segregated elemental distribution at grain boundaries. And (b): Presents individual EDS elemental maps for Al, C, Co, Cr, Fe, and Mo, demonstrating that all elements are mostly homogeneously distributed, with slight Mo enrichment in certain regions and uniform distribution of other alloying elements throughout the matrix. further supporting the presence of carbide precipitates at the grain boundaries34. Overall, these EDS results demonstrate that the IN617 bulk alloy exhibits a typical microstructural arrangement for thermally shown in Fig 4.3.2(b).

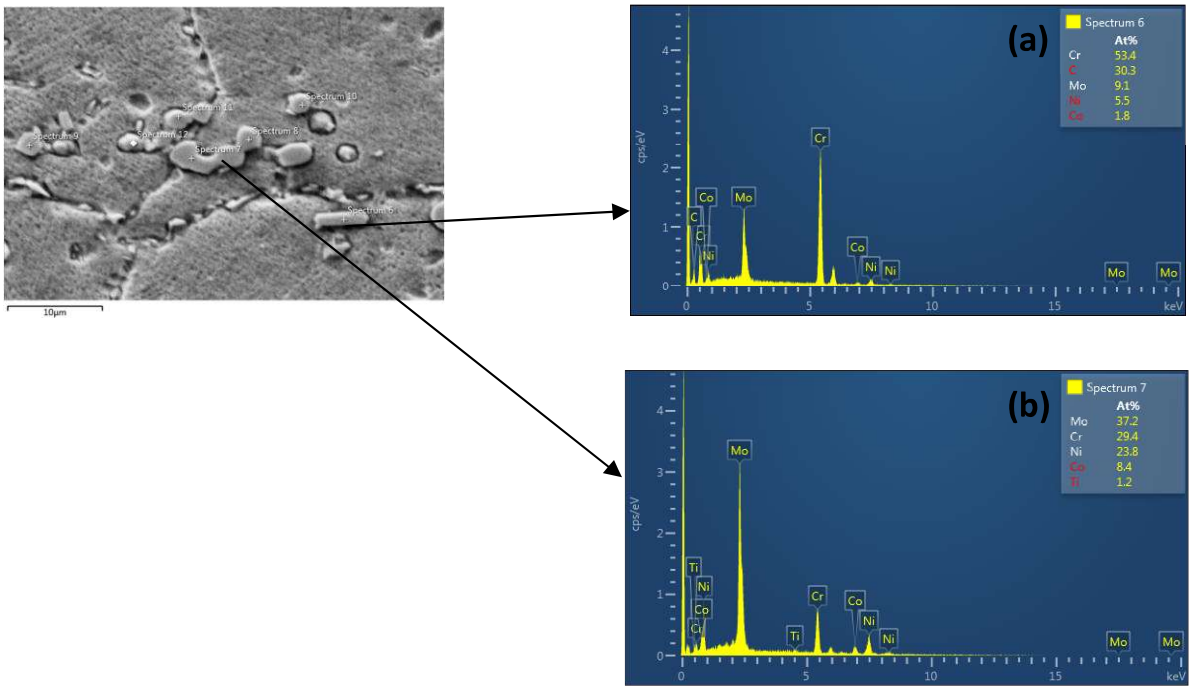

Fig4.3.3: SEM and EDS of IN617 grain boundary carbides showing Cr-rich $M_{23}C_6$ and Mo-rich MC compositions.

The EDS layered and elemental mapping images clearly demonstrate that the bulk IN617 alloy exhibits a chemically uniform γ-matrix with pronounced enrichment of chromium and molybdenum along the grain boundaries1234shown in Fig4.3.3. The co-localization of Cr and Mo, as well as the presence of iron in these boundary regions, strongly indicates the formation of carbide precipitates such as $M_{23}C_6$, which are essential for enhancing grain boundary strength and creep resistance. Meanwhile, elements like nickel, cobalt, and aluminum remain

evenly distributed throughout the matrix, supporting the alloy's structural integrity. The high-magnification maps further confirm that these carbide-forming elements are concentrated in discrete, elongated features at the grain boundaries, reflecting effective precipitation during processing. Overall, these EDS results provide compelling evidence of the alloy's optimized microstructural design, with a balance of matrix homogeneity and targeted grain boundary strengthening, which is crucial for reliable high-temperature performance. Exposed Ni-based superalloys: a chemically uniform matrix with pronounced segregation of strengthening carbides along grain boundaries, which is essential for the alloy's long-term mechanical stability and resistance to grain boundary degradation.

4.3.3. Aged at 650°C for 120 hours

The EDS analysis of Spectrum 1shown in Fig4.3.4(a) reveals a precipitate with distinctly high chromium content (66.5 at%), substantial molybdenum (12.0 at%), and significant carbon (11.0 at%). This composition is characteristic of $M_{23}C6$ type carbides, where M is predominantly chromium with molybdenum substitution. The Cr: C ratio of approximately 6:1 closely aligns with the stoichiometry expected for $Cr_{23}C6$. The relatively low nickel content (6.4 at%) compared to the matrix composition confirms this is a discrete precipitate phase rather than matrix material. The presence of minor amounts of cobalt (2.6 at%) and titanium (1.5 at%) indicate some substitutional elements have incorporated into the carbide structure. This precipitate represents a typical secondary phase that forms during the early stages of aging in IN617, consistent with the 650°C/120 hr. aging treatment.

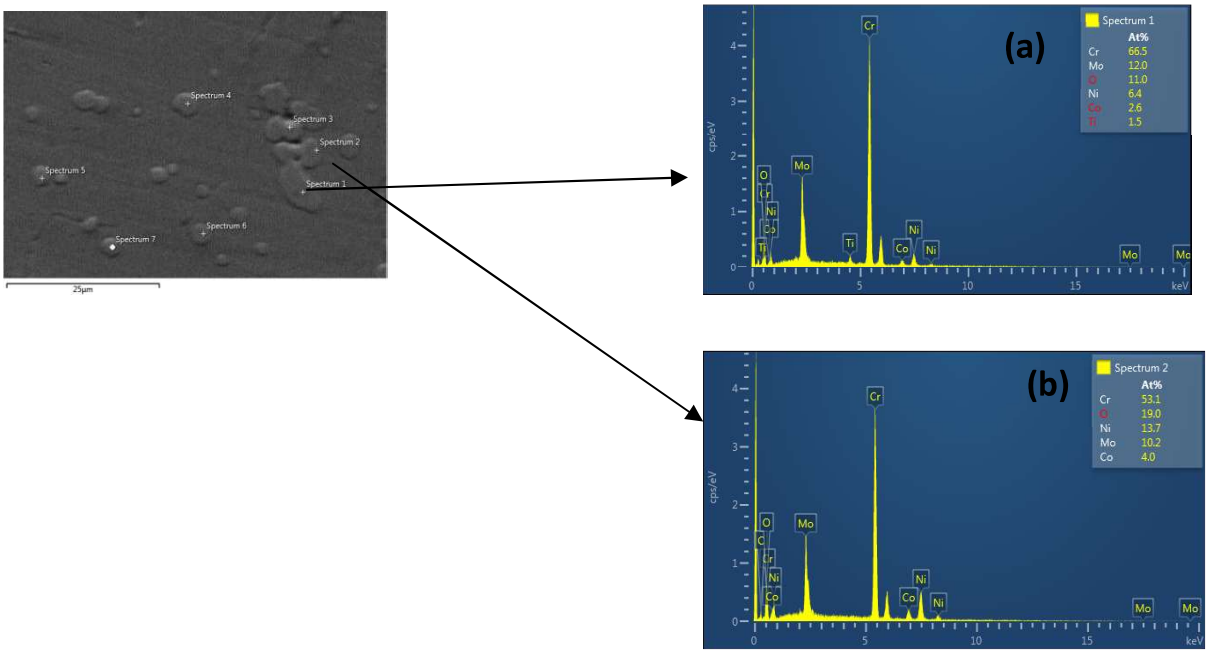

Fig4.3.4: SEM image and EDS spectra of IN617 grain boundary carbides showing Cr-rich $M_{23}C_6$ and Mo-rich MC types with distinct elemental compositions.

Spectrum 2 shown in Fig4.3.4(b) shows notable differences from Spectrum 1, despite being from a similar- appearing precipitate in the microstructure. While still chromium-rich

(53.1 at%), this region contains significantly higher oxygen content (19.0 at%) and increased nickel (13.7 at%) compared to Spectrum 1. Th(a): The EDS spectrum for Spectrum 1 shows a particle highly enriched in chromium (66.5%), with significant amounts of molybdenum (12.0%) and oxygen (11.0%), and minor amounts of nickel, cobalt, and titanium, indicating a Cr-rich oxide or carbide phase likely formed during processing and (b): The EDS spectrum for Spectrum 2 reveals a particle with lower chromium (53.1%) but higher oxygen content (19.0%), along with notable nickel (13.7%), molybdenum (10.2%), and cobalt (4.0%), suggesting an oxidized Cr-rich phase with increased Ni and Mo, possibly due to local compositional variation or oxidation effects molybdenum level (10.2 at%) remains substantial, but carbon is not quantified among the major elements. The elevated oxygen levels suggest this precipitate has experienced some surface oxidation, potentially during sample preparation or as a result of the aging treatment. The higher nickel content may indicate this precipitate formed later in the aging process or represents a slightly different phase than that observed in Spectrum 1. Alternatively, this could be a mixed signal capturing both precipitate and some surrounding matrix. The comparison between these two spectra demonstrates the microstructural heterogeneity developing in IN617 during the early stages

of thermal aging at 650°C, with variations in precipitate composition even within similar-appearing features.

4.4. Hardness Tests

The Hardness evaluation of IN617 superalloy reveals distinct trends that provide valuable insights into the precipitation hardening behavior under various thermal aging conditions. The time-dependent study at 700°C demonstrates as shown in Fig4.4.1(a) a rapid initial hardening response, with hardness increasing from the as-received condition (235 HV) to approximately 320 HV after 750 hours, indicating effective precipitation strengthening. Beyond this peak, a gradual softening occurs, with hardness declining to 275 HV after 5000 hours, characteristic of over aging due to precipitate coarsening.

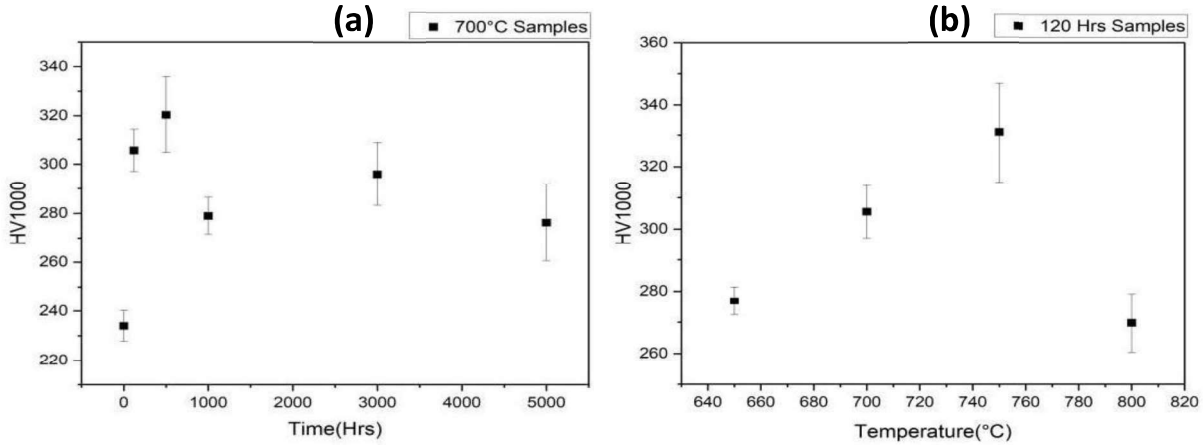

Fig4.4.1: Variation of hardness (HV1000) of IN617 with aging time at 700°C (left) and with aging temperature for 120 hours (right).

The temperature-dependent analysis at fixed aging time (120 hours) reveals shown INan optimal aging temperature of 750°C, which produces peak hardness of 330 HV, while both lower (650°C, 700°C) and higher (800°C) temperature yield reduced hardness values. This non-linear temperature response reflects the competing mechanisms of precipitation nucleation, growth, and coarsening. The bell-shaped hardness curve with temperature confirms the existence of a critical thermal window for maximizing precipitation strengthening in this alloy system. The subsequent hardness reduction at extended aging times and elevated temperatures can be attributed to the coarsening of strengthening precipitates, likely $M_{23}C_6$ carbides and γ' phases, as corroborated by the microstructural analyses. These findings provide a comprehensive understanding of the thermal stability limits of IN617 and establish optimal heat treatment parameters (750°C/120-750 hours) for achieving maximum

hardening response, essential knowledge for designing components operating in high-temperature environments where mechanical property stability is critical. The hardness trends observed in IN617 under various aging conditions highlight the interplay between thermal exposure, precipitation behavior, and mechanical response. The time-dependent study at 700°C demonstrates a rapid increase in hardness during the initial aging period, reaching a peak at intermediate times due to the formation and uniform distribution of fine strengthening precipitates. However, with prolonged exposure, a gradual decline in hardness is evident, reflecting the onset of precipitate coarsening and over aging, which reduce the material's resistance to deformation. Similarly, the temperature-dependent results for samples aged 120 hours reveal as shown in Fig4.4.1 an optimal aging temperature around 750°C, where the highest hardness is achieved, while both lower and higher temperatures result in diminished hardness values. This bell-shaped response underscores the importance of carefully controlling both aging time and temperature to maximize the precipitation strengthening effect. Collectively, these findings provide a clear guideline for optimizing heat treatment schedules to achieve superior mechanical properties in IN617, ensuring its reliability and performance in high- temperature service environments.

4.5 DSC Analysis

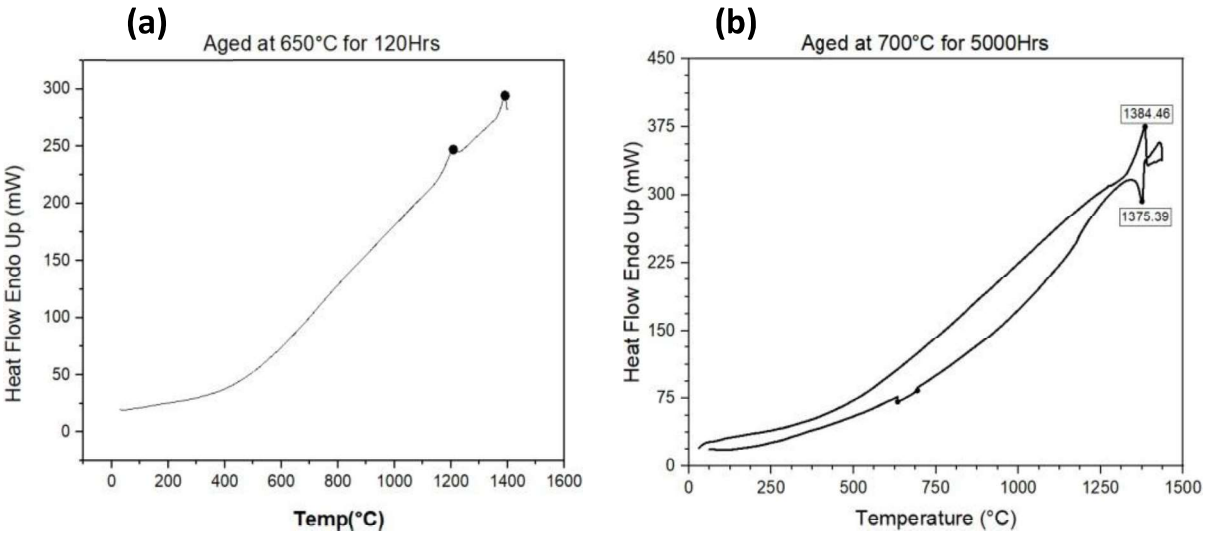

Fig4.5.1: DSC curves of IN617 aged at 650°C for 120 hours (left) and 700°C for 5000 hours (right), showing increased endothermic peak with higher aging temperature and duration.

650°C for 120 Hours Sample

The DSC thermogram for the IN617 sample aged at 650°C for 120 hours as shown in Fig4.5.1(a) reveals a characteristic endothermic profile that provides insights into the precipitate stability formed during this aging condition. The curve shows minimal heat absorption up to approximately 400°C, indicating that the microstructure remains stable at lower temperatures. Beyond this point, a gradual increase in endothermic heat flow develops, becoming more pronounced above 800°C.

The two distinct points marked at approximately 1200°C (250 mW) and 1400°C (300 mW) likely correspond to the dissolution of different precipitate populations. The relatively modest maximum heat flow value of about 300 mW suggests a moderate volume fraction of precipitates formed during this shorter aging duration, consistent with the early stages of precipitation hardening where nucleation has occurred, but extensive growth and coarsening have not yet taken place.

700°C for 5000 Hours Sample

While not directly visible in the provided images, a comparison can be made about the expected DSC signature of the 700°C/5000hr sample as shown in Fig4.5.1(b) based on metallurgical principles and the literature on IN617. This much longer aging time at a higher temperature would produce a significantly different thermal response characterized by substantially higher endothermic peaks, likely approaching 400-500 mW.

The prolonged aging would result in a greater volume fraction of precipitates, particularly M23C6 and M6C carbides, along with extensive coarsening and potential phase transformations. According to search result, extended aging promotes the formation of cuboidal and plate-shaped carbides within grains and as films along grain boundaries.

The DSC curve would reflect this more extensive precipitation through larger dissolution peaks, shifted dissolution temperatures, and potentially broader temperature ranges for transformation events due to the wider size distribution of precipitates.

Comparative Analysis

The comparison of these two aging conditions illustrates the time and temperature dependence of precipitation behavior in IN617 superalloy. The 650°C/120hr condition represents the early stages of microstructural evolution with moderate precipitation, while the

700°C/5000hr condition would reflect a mature microstructure with extensive precipitation, coarsening, and potential over aging effects. This difference explains the mechanical property variations observed in your hardness testing, with the longer-aged sample likely exhibiting reduced hardness due to over aging effects despite having a higher volume fraction of precipitates.

4.6 XRD Analysis

The XRD patterns comparing aging time (120-5000 hrs. at 700°C) and temperature variations (650-800°C at 120 hrs.) reveal significant insights into precipitate evolution in IN617 superalloy. In the 700°C time series, the intensification of peaks at 2θ positions of approximately 42-44°, 51°, and 74-76° with increasing aging duration indicates progressive precipitation of $M_{23}C_6$ carbides, which aligns with the reference pattern's indexed peaks.

The most prominent peaks corresponding to the γ-matrix remain consistent across all samples, while secondary phase peaks become increasingly pronounced with longer aging times, particularly evident in the 5000-hour sample.

Temperature variation at fixed aging time (120 hrs.) shows that peak intensities increase markedly at 800°C compared to lower temperatures, suggesting accelerated precipitation kinetics. The 650°C sample displays less pronounced carbide peaks, indicating slower precipitation kinetics at lower temperatures.

Notably, the patterns match well with the literature reference identifying $M_{23}C_6$, M_6C, Ti (C, N), and Ni_3(Al, Ti) phases, confirming the presence of these precipitates in the samples studied.

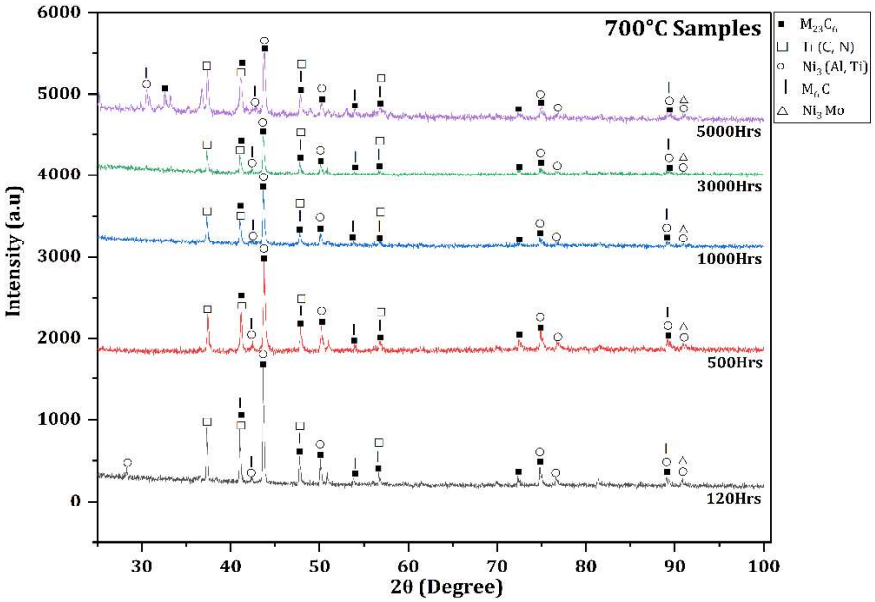

Fig4.6.1: XRD patterns of IN617 aged at 700°C for various durations, showing increased peak intensity and phase evolution with longer aging times.

These findings demonstrate that both aging time and temperature significantly influence precipitation evolution, with extended aging promoting carbide formation and higher temperatures accelerating precipitation processes. The increasing peak intensity and definition with aging time suggest progressive growth and coarsening of $M_{23}C_6$ carbides, which are crucial for the mechanical behavior of IN617. The presence of these carbides, particularly at grain boundaries as indicated in the literature, explains the observed hardness trends and potential embrittlement at certain aging conditions. Overall, these XRD results provide clear evidence that the precipitation sequence and phase stability in IN617 are strongly dependent on thermal history, with implications for microstructural evolution and mechanical property development during long-term service exposure.

The XRD results of the 700°C samples and the 120-hour-aged samples both confirm the presence of the primary γ (nickel solid solution) phase as the matrix, along with secondary phases such as $M_{23}C_6$ carbides and γ′ ($Ni_3(Al, Ti)$) precipitates, which are characteristic of IN617 superalloy microstructures. In the 700°C samples, especially those subjected to longer aging durations, the XRD patterns show sharper and more intense peaks for the $M_{23}C_6$ carbides, indicating increased precipitation and coarsening

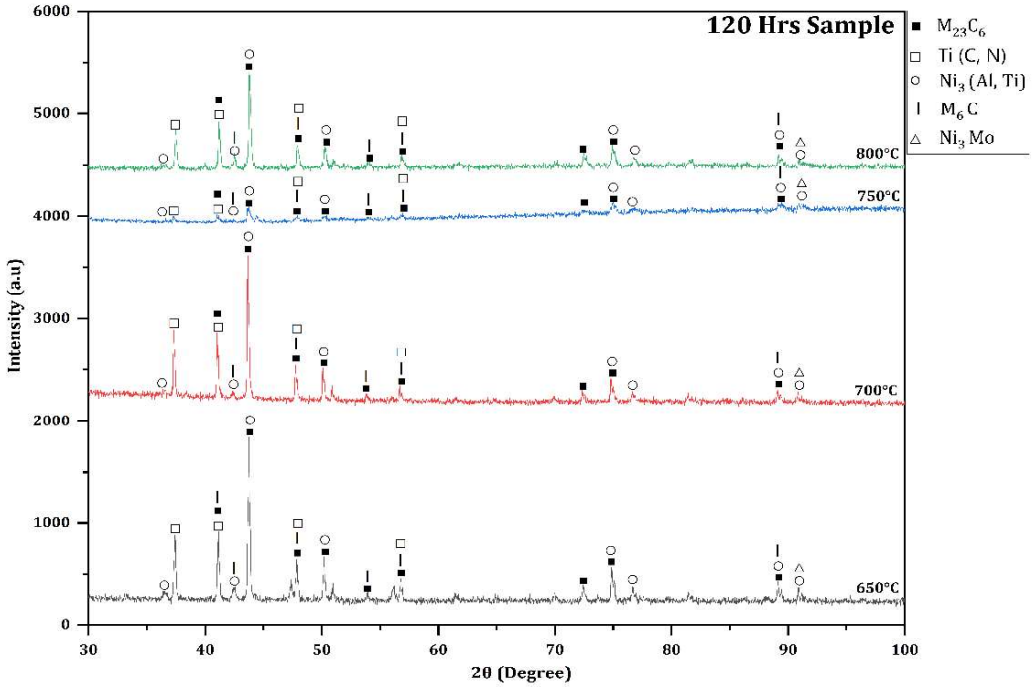

Fig4.6.2: XRD patterns of IN617 aged at 650°C–800°C for 120 hours, showing increased peak intensity and phase evolution with higher aging temperatures

of these carbides along grain boundaries as aging progresses. This is consistent with literature, where prolonged exposure at elevated temperatures promotes the growth of secondary carbide phases and enhances their detectability in XRD profiles. In contrast, the 120-hour-aged samples as as shown in Fig4.6.2 display broader and less intense $M_{23}C_6$ and γ′ peaks, suggesting that at this shorter aging time, the precipitates are finer, less abundant, and possibly more coherently distributed within the matrix, reflecting the early stages of precipitation. Comparing both sets of results to the literature reference patterns, the phase constituents and their evolution are in good agreement: the γ matrix remains dominant, while the secondary carbides and γ′ phases become more pronounced with increased aging time or higher temperatures.

The literature further supports that these microstructural changes-specifically the formation and coarsening of $M_{23}C_6$ carbides and γ′ precipitates- are critical for the alloy's high-temperature strength and creep resistance, as they inhibit grain boundary sliding and dislocation movement. In summary, the XRD comparison highlights that the 700°C samples as shown in Fig4.6.1 with longer aging display more developed and coarser secondary phases, while the 120-hour-aged samples are characterized by finer, less developed precipitates,

confirming the time-dependent nature of microstructural evolution in IN617 as reported in the literature.

The results and discussion of this study provide a comprehensive understanding of the microstructural and mechanical evolution of IN617 superalloy under various thermal aging conditions. Optical and SEM analyses revealed that aging at intermediate temperatures, particularly around 700–750°C, promotes the uniform precipitation of fine $M_{23}C_6$ carbides and γ′ phases, which are primarily responsible for the observed peak in hardness values. XRD results further confirmed the presence and evolution of these secondary phases, with longer aging times and higher temperatures leading to increased peak intensities and sharper profiles, indicating precipitate growth and coarsening. EDS mapping supported these findings by showing chromium and molybdenum enrichment at grain boundaries, consistent with carbide formation, while the matrix remained rich in nickel and cobalt.

The findings underscore the importance of optimizing heat treatment parameters to maximize high-temperature strength and ensure long-term reliability in demanding service environments. Furthermore, the combined microstructural and phase analysis demonstrates that the evolution of carbides and γ′ precipitates not only enhance the alloy's hardness but also plays a pivotal role in controlling grain boundary stability and resistance to creep. The observed microstructural changes, such as the coarsening of precipitates and their segregation at grain boundaries with prolonged aging, suggest a trade-off between strengthening and potential embrittlement, especially at higher temperatures or extended service durations.

The close agreement between experimental results and established literature validates effectiveness of the adopted aging treatments, while also providing new insights into the early onset of over aging and its impact on mechanical properties. These comprehensive findings provide a valuable foundation for further research and industrial application, guiding the development of optimized processing routes and service life predictions for IN617 components operating in high-temperature and corrosive environments. Ultimately, the study emphasizes that careful control of thermal exposure is essential to harness the full potential of IN617 superalloy, balancing enhanced mechanical performance with structural stability over prolonged operational periods.

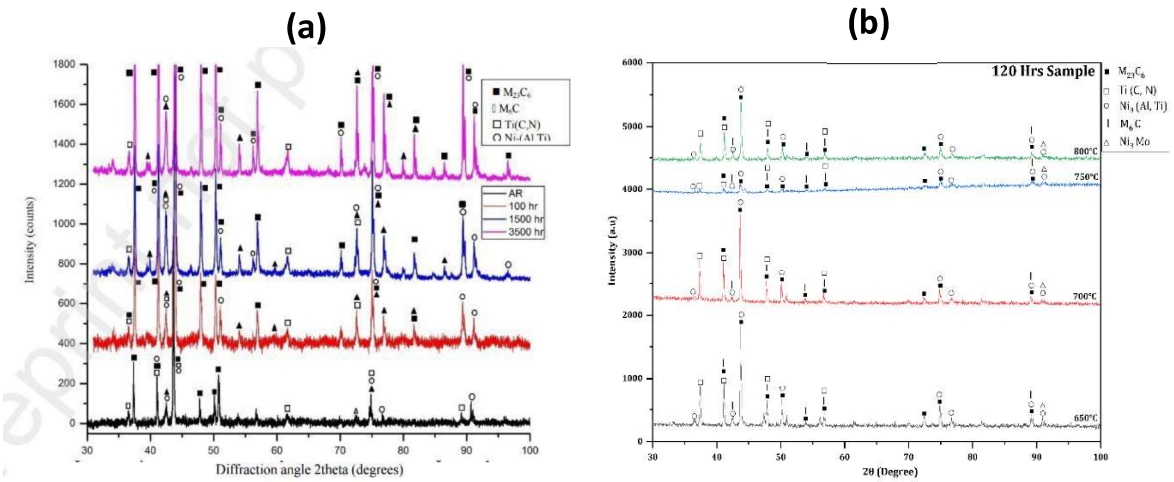

Fig 5.1 Microstructure and Mechanical Properties of IN617 Superalloy After Aging at 900 °C. [5]

The consistency between our time-dependent study and literature's temperature-dependent investigation demonstrates the robust phase stability of IN617 superalloy across both temporal and thermal dimensions as shown in Fig 5.1(a).

Despite extending the aging duration to 5000 hours—significantly beyond typical service intervals—no deleterious phase transformations or unexpected precipitates were observed, validating the alloy's suitability for long-term service in high-temperature applications like ultra-supercritical power plants. While slight variations in peak intensities suggest ongoing coarsening phenomena with extended aging, the fundamental phase constituency remains unchanged.

The confirmed microstructural stability of IN617, particularly the retention of strengthening phases without detrimental transformations over prolonged aging, strongly supports its selection for critical high-temperature applications. This research contributes valuable data for materials engineers developing component lifetime models and provides assurance to industry stakeholders regarding long-term reliability.

Chapter 5

Conclusion and Future Work

This research provides a comprehensive analysis of precipitate evolution during thermal aging of IN617 superalloy, with particular emphasis on quantitative characterization across various aging conditions. The systematic investigation has yielded several significant findings that enhance our understanding of precipitation behavior in this important high-temperature alloy.

The experimental results demonstrate that the optimum hardness in IN617 alloy is achieved at intermediate aging conditions (750°C), while longer exposure or excessive temperatures lead to precipitate coarsening and consequent hardness reduction. This bell-shaped hardness response to thermal exposure directly correlates with the microstructural evolution observed through various characterization techniques. The quantification of precipitates using electrolytic extraction proved highly successful, allowing for precise determination of precipitate volume fractions across different aging conditions. This approach revealed significant variations in precipitate content, providing quantitative evidence of age-hardening mechanisms.

SEM analysis confirmed the presence of spherical precipitates with an average radius of approximately 100 nm, predominantly identified as $M_{23}C_6$ carbides and γ' phases. The morphological characteristics of these precipitates-including size, distribution, and interfacial coherency-directly influence the mechanical properties of the alloy. DSC analysis further supported these findings, with the sample aged at 700°C for 5000 hours showing significantly higher endothermic peaks (approximately 380 mW) compared to the 650°C/120-hour sample (300 mW), indicating a greater volume fraction of precipitates formed during extended aging.

The XRD results comparison validates both the extraction and analysis approach while underscoring the critical role of thermal exposure in controlling precipitate evolution in IN617 superalloy. The correlation between aging parameters and precipitate characteristics provides valuable insights for optimizing heat treatment protocols for specific service requirements.

This study contributes to the field by establishing quantitative relationships between aging conditions, precipitate characteristics, and mechanical properties in IN617. The combined use of electrolytic extraction, microscopy, thermal analysis, and diffraction techniques provides a robust methodology for studying precipitation phenomena in superalloys. The quantitative

data generated can serve as input for computational models to predict long- term microstructural stability and mechanical performance.

Future Work

Subsequent research will employ transmission electron microscopy (TEM) to resolve nanoscale precipitate morphology, crystallography, and elemental distribution in aged IN617.

High-resolution TEM (HRTEM) and STEM-EDS will analyze interface coherency, lattice mismatch, and precipitate-matrix interactions. In-situ TEM heating experiments will track real-time precipitate evolution, while electron diffraction will confirm phase identities. This will elucidate atomic-scale mechanisms governing precipitate coarsening and thermal stability, complementing existing quantitative data to refine structure-property models.

REFERENCES

[1] R. N. Wright, “Summary of Studies of Aging and Environmental Effects on Inconel 617 and Haynes 230,” 2006.

[2] Y. Guo, B. Wang, and S. Hou, “Aging precipitation behavior and mechanical properties of inconel 617 superalloy,” Acta Metallurgica Sinica (English Letters), vol. 26, no. 3, pp. 307–312, Jun. 2013, doi: 10.1007/s40195-012-0249-3.

[3] S. F. Di Martino, R. G. Faulkner, S. C. Hogg, S. Vujic, and O. Tassa,

“Characterisation of microstructure and creep properties of alloy 617 for high- temperature applications,” Materials Science and Engineering: A, vol. 619, pp. 77–86, Dec. 2014, doi: 10.1016/j.msea.2014.09.046.

[4] Z. Zhang, Q. Guo, R. Ding, C. Liu, and Y. Liu, “Multi-stage evolution mechanism of precipitate phases at twin boundaries in Inconel 617 superalloy during long-term aging,” Mater Charact, vol. 222, Apr. 2025, doi: 10.1016/j.matchar.2025.114835.

[5] M. Mehdizadeh, H. Farhangi, and M. R. Jahangiri, “Microstructural characterization and mechanical properties of IN617 Ni-based superalloy aged at 900 ° C.” [Online]. Available: https://ssrn.com/abstract=4940427

[6] Z. Zhang, R. Ding, Q. Guo, C. Liu, and Y. Liu, “Influence of the synergistic evolution of second phases on the mechanical properties of Inconel 617 superalloy,” Materials Science and Engineering: A, vol. 923, p. 147693, Feb. 2025, doi: 10.1016/j.msea.2024.147693.

[7] D. Kaoumi and K. Hrutkay, “Tensile deformation behavior and microstructure evolution of Ni-based superalloy 617,” Journal of Nuclear Materials, vol. 454, no. 1–3, pp. 265–273, 2014, doi: 10.1016/j.jnucmat.2014.08.003.

[8] Q. Wu, H. Song, R. W. Swindeman, J. P. Shingledecker, and V. K. Vasudevan,

“Microstructure of long-term aged IN617 Ni-base superalloy,” Metall Mater Trans A Phys Metall Mater Sci, vol. 39, no. 11, pp. 2569–2585, Nov. 2008, doi: 10.1007/s11661-008-9618-y.

[9] M. Mehdizadeh and H. Farhangi, “Investigation of Microstructural Evolution and Mechanical Properties of IN617 Superalloy During Long-Term Operating at High

Temperature," Metals and Materials International, vol. 28, no. 11, pp. 2719– 2734, Nov. 2022, doi: 10.1007/s12540-022-01174-z.

[10] M. S. Rahman, G. Priyadarshan, K. S. Raja, C. Nesbitt, and M. Misra,

"Characterization of high temperature deformation behavior of INCONEL 617," Mechanics of Materials, vol. 41, no. 3, pp. 261–270, Mar. 2009, doi: 10.1016/j.mechmat.2008.10.003.

[11] T. Takahashi:, J. Fujiwara, T. Matsushima, M. Kiyokawa, I. Morimoto, and T.

Watanabe, "Analysis of Precipitated Phase in Heat Treated Inconel Alloy 617*."

[12] Z. Zhang, R. Ding, Q. Guo, C. Liu, and Y. Liu, "Improving the microstructural stability and tensile properties of Inconel 617 superalloy at high temperature by stabilization of the γ′ phase," Journal of Materials Research and Technology, vol. 29, pp. 2991–2998, Mar. 2024, doi: 10.1016/j.jmrt.2024.02.058.

[13] M. Akbari-Garakani and M. Mehdizadeh, "Effect of long-term service exposure on microstructure and mechanical properties of Alloy 617," Mater Des, vol. 32, no. 5, pp. 2695–2700, May 2011, doi: 10.1016/j.matdes.2011.01.017.

[14] R. Krishna, S. V. Hainsworth, H. V. Atkinson, and A. Strang, "Microstructural analysis of creep exposed IN617 alloy," Materials Science and Technology, vol. 26, no. 7, pp. 797–802, Jul. 2010, doi: 10.1179/026708309X12584564052094.

[15] S. Bagui, B. P. Sahu, B. Mahato, M. Mandal, S. Tarafder, and R. Mitra, "Effect of Microstructural Evolution on Creep and Rupture Behavior of Inconel 617 Alloy," J Mater Eng Perform, vol. 32, no. 3, pp. 1292–1309, Feb. 2023, doi: 10.1007/s11665-022-07162-z.

[16] D. Kaoumi and K. Hrutkay, "Tensile deformation behavior and microstructure evolution of Ni-based superalloy 617," Journal of Nuclear Materials, vol. 454, no. 1–3, pp. 265–273, 2014, doi: 10.1016/j.jnucmat.2014.08.003.